The Lifetime of Insulin Hexamers

Ulrich Hassiepen, Matthias Federwisch, Thomas Mülders, and Axel Wollmer

Institut für Biochemie, Rheinisch-Westfälische Technische Hochschule Aachen, 52057 Aachen, Germany

ABSTRACT The kinetic stability of insulin hexamers containing two metal ions was investigated by means of hybridization experiments. Insulin was covalently labeled at the N_ε-amino group of Lys^{B29} by a fluorescence donor and acceptor group, respectively. The labels neither affect the tertiary structure nor interfere with self-association. Equimolar solutions of pure donor and acceptor insulin hexamers were mixed, and the hybridization was monitored by fluorescence resonance energy transfer. With the total insulin concentration remaining constant and the association/dissociation equilibria unperturbed, the subunit interchange between hexamers is an entropy-driven relaxation process that ends at statistical distribution of the labels over 16 types of hexamers differing by their composition. The analytical description of the interchange kinetics on the basis of a plausible model has yielded the first experimental values for the lifetime of the hexamers. The lifetime is reciprocal to the product of the concentration of the exchanged species and the interchange rate constant: $\tau = 1/(c \cdot k)$. Measured for different concentrations, temperatures, metal ions, and ligand-dependent conformational states, the lifetime was found to cover a range from minutes for T_6 to days for R_6 hexamers. The approach can be used under an unlimited variety of conditions. The information it provides is of obvious relevance for the handling, storage, and pharmacokinetic properties of insulin preparations.

INTRODUCTION

Evolution has shaped proinsulin for self-association. At the high concentration existing in the storage granules of the β-cells and in the presence of zinc and calcium ions, hexamers are formed with two Zn^{2+} ions and probably one Ca^{2+} ion specifically coordinated (Palmieri et al., 1988). Tied up in the hexamer, cleavage sites within the insulin moiety are protected from the enzymes converting proinsulin to insulin. Whereas the highly flexible C-peptides on the outside of the hexamers prevent proinsulin from crystallization, crystals are readily formed by the insulin hexamers after the C-peptide has been cleaved off (Dodson and Steiner, 1998). Both hexamer and microcrystal formation reduce the numerical concentration in the granule, protecting it from osmotic threat.

Self-association also has a key role with respect to insulin preparations for therapy. It is essentially the hexameric state that provides the stability required for long shelf-life (Brange, 1994). Hexamerization is promoted by the addition of Zn^{2+} ions or other divalent transition metals (Schlichtkrull, 1958). Metal-bound hexamers are known to exist in essentially three conformational states, T_6, T_3R_3, and R_6 (for the nomenclature see Kaarsholm et al., 1989), all defined by x-ray crystallography (Baker et al., 1988; Bentley et al., 1976; Derewenda et al., 1989; Smith and Dodson, 1992). In solution these states are related by dynamic equilibria that can be shifted from T_6 to T_3R_3 by the addition of

inorganic anions (Bentley et al., 1975; De Graaf et al., 1981; Renscheidt et al., 1984; Ramesh and Bradbury, 1986; Kaarsholm et al., 1989) or adequately moderate concentrations of phenol-like molecules (Wollmer et al., 1987; Roy et al., 1989; Krüger et al., 1990; Gross and Dunn, 1992). Higher concentrations of the latter can shift the conformational state completely to R_6: $T_6 \leftrightarrow T_3R_3 \leftrightarrow R_6$ (Wollmer et al., 1987; Roy et al., 1989; Thomas and Wollmer, 1989; Krüger et al., 1990), which further stabilizes the hexamer.

The pharmacodynamics and pharmacokinetics of insulin are determined by the diffusion rate from the injection site into the blood and, hence, are crucially dependent on the particle size. Therefore, the modification of any factors, intrinsic or extrinsic, that influence the solubility and dissociation of insulin crystals, precipitates, or aggregates is the main approach to optimizing the therapeutic action profile according to physiological one.

The aim of the work reported here was to study the kinetic stability of insulin hexamers by means of hybridization experiments. The formation of hybrid associates has been exploited for manifold purposes, for instance to determine the number of polypeptide chains in oligomeric proteins (Meighen et al., 1970), to relate activity to the quaternary structural state (Jaenicke et al., 1971), to evaluate the strength of interactions between subunits (Anderson and Weber, 1966; Yang and Schachman, 1987; Eisenstein and Schachman, 1989), or to follow subunit exchange between isoenzymes or reassociation superimposed by conformational drift (Erijman and Weber, 1991, 1993) or folding processes (Jaenicke and Rudolph, 1986; Jaenicke, 1987). To our knowledge this is the first time that the approach has been applied to hexamers and, more specifically, to insulin hexamers.

To monitor hybridization, we use fluorescence resonance energy transfer (FRET) (Förster, 1948) from insulin molecules labeled with a donor to insulin molecules labeled with

an acceptor (Erijman and Weber, 1993; Price, 1994). The 2-aminobenzoyl group serves as the fluorescence donor and 3-nitro-tyrosyl chromophore as the acceptor. Both labels were attached covalently via peptide bonds to the exposed N_ε amino group of Lys^{B29}, yielding donor insulin, I_d, and acceptor insulin, I_a, respectively (Fig. 1 *A*). The labels were shown neither to affect the tertiary structure nor to interfere with self-association, and, hence, I_d and I_a are representative of the native hormone (Hassiepen et al., 1998). Energy transfer from the donor group to the quenching acceptor group only occurs when I_d and I_a coexist as subunits in the very same hexamer. Therefore the decrease in fluorescence

emission observable with the mixing of solutions of pure I_d and pure I_a hexamers, respectively, reflects the interchange of subunits between the hexamers. As equimolar solutions are mixed, the interchange takes place as an entropy-driven relaxation process, with the overall insulin concentration remaining constant and the association/dissociation equilibria unperturbed.

The experimental time course of the interchange can be described by a model based on plausible assumptions about the molecular species actually exchanged between the hexamers. The fit is optimized by the adjustment of a single parameter, which is the lifetime of the hexamers.

FIGURE 1 (*A*) Distribution of the labels for fluorescence energy transfer in the 2Zn insulin hexamer, attached to the ε-amino group of Lys^{B29} (*large spheres*), and view perpendicular to the threefold axis carrying the zinc ions (*small spheres*). Coordinates: PDB 2INS (Smith et al., 1982). Graphics: GRASP (Nicholls et al., 1991). (*B*) Schematic projection of the hexamer along the threefold axis, with the numbers serving to designate the distance between the N_ε atoms of Lys^{B29} (see Table 1). Full lines: upper trimer; broken lines: lower trimer.
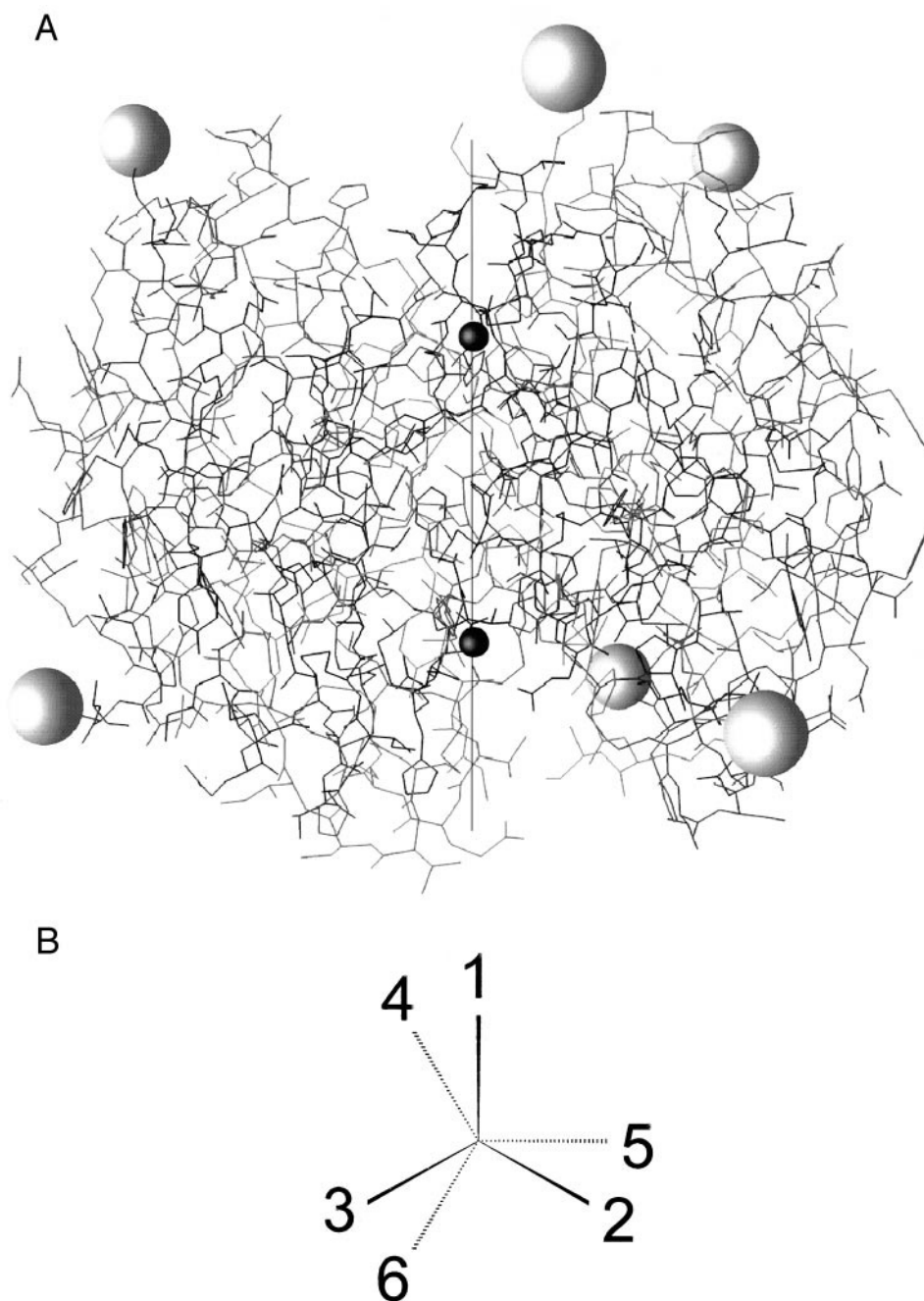
MATERIALS AND METHODS

Reagents and solvents

All reagents and solvents were of analytical grade and are commercially available. Porcine N_ϵ^{B29}-2-aminobenzoyl-insulin (N_ϵ^{B29}-Abz-insulin, I_d) carrying the fluorescence donor group (d) and porcine N_ϵ^{B29}-3-nitro-L-tyrosyl-insulin (N_ϵ^{B29}-Tyr(NO$_2$)-insulin, I_a) carrying the acceptor group (a) were prepared as described earlier (Lenz et al., 1994; Hassiepen et al., 1998).

Solutions for spectroscopy

The solvent for insulin used was 25 mM Tris/HCl buffer (pH 7.8) or aqua bidest. In the latter case the pH was adjusted by NaOH or HCl.

Insulin concentrations c_d and c_a were determined photometrically using a Cary 1Bio UV/visible spectrophotometer (Varian GmbH, Darmstadt, Germany). The molar extinction coefficients at 276 nm used were $\epsilon_d = 7090$ M^{-1} cm^{-1} for I_d and $\epsilon_a = 11,000$ M^{-1} cm^{-1} for I_a (Hassiepen et al., 1998).

Fluorescence spectroscopy

All fluorescence measurements were made on a Spex Fluorolog 211 photon counting spectrometer (Spex Instruments S.A., Stanmore, UK). The system provides corrections for changes in the lamp intensity and for the spectral sensitivity of the emission monochromator and photomultiplier. Modifications made to achieve long-term stability were described by Hassiepen et al. (1998).

The excitation wavelength for the Abz fluorophore was 330 nm throughout. The spectral bandwidth was 1.8 nm on both the excitation and emission sides.

The stopped-flow accessory used for the kinetic experiments was built in the workshop of the Institute, except for the mixer/optical cell/stopper unit, which was taken from a prototype of the AVIV 63SF spectrometer (Aviv Instruments, Lakewood, NJ) and mounted on the Spex Fluorolog. The dimensions of the cell were 1 mm in the direction of the excitation beam and 2 mm in the direction of the emission. The solution reservoirs, the syringes, and the cell holder were temperature controlled by circulating water. The syringes were actuated by compressed air. The measurements were carried out at 20°C unless stated otherwise. Equal volumes of equimolar solutions of I_d and I_a were mixed. The changes in the intensity at the fluorescence maximum of the donor were used to follow the kinetics.

The reaction between *N*-bromosuccinimide and *N*-acetyltryptophana-mide (Peterman, 1979) was used to determine the dead time of the stopped-flow instrument under our experimental conditions, which was ∼25 ms, thus allowing reactions with rate constants smaller than 40 s^{-1} to be followed.

Kinetics were measured three times under identical conditions and averaged. Single exponentials were fitted to the curves by the software package ORIGIN (Microcal Software, Northampton, MA). The computer algebra program MAPLE V Release 5.1 (Waterloo Maple, Waterloo, ON, Canada) was used to solve the differential equations.

RESULTS AND DISCUSSION

To follow the interchange of subunits between insulin hexamers by fluorescence resonance energy transfer (FRET), the hormone had to be covalently labeled. The aminobenzoyl (Abz) donor group as well as the nitrotyrosyl (Tyr(NO$_2$)) acceptor group, respectively, were attached to the ε-amino group of Lys^{B29}. Owing to their exposed position also in the hexamer (see Fig. 1 *A*), the labels do not interfere with the assembly of the quaternary structure, as demonstrated in a previous report (Hassiepen et al., 1998). This circumstance, together with the fact that FRET only occurs between donors and acceptors within the very same hexamer, is essential for the present study.

By mixing equal volumes of equimolar solutions of pure donor insulin (I_d) and acceptor insulin (I_a) hexamers, respectively, so that the total concentration remains constant and the association/dissociation equilibria are unperturbed, an entropy-driven process is started that ends in a steady state of statistical distribution of I_d and I_a over the hexamers. Although the volumes of I_d and I_a mixed are, of course, free to be varied, the experiments as well as the theoretical analyses reported here refer to 1:1 mixtures without exception. The analysis of the time course of the process under different experimental conditions requires the steady state to be analyzed beforehand.

Analysis of the energy transfer in the steady state

In the schematic projection of the insulin hexamer along the threefold axis (Fig. 1 *B*), the positions of the N_ϵ^{B29} atoms are represented by the numbers 1–6. The distance between any two of these atoms (Table 1) is known from the x-ray structure of 2Zn porcine insulin (Baker et al., 1988). Because of the hexamer symmetry, only four different distances exist.

Seven classes of hexamers are distinguished by the number of donor or acceptor subunits, respectively, they contain (see Table 2). Owing to equal homo- and heterodissociation/association properties of I_d and I_a (Hassiepen et al., 1998), the equilibrium distribution of donors and acceptors will be binomial, and the probability of finding a hexamer with k donors is given by

$$P_k = \binom{6}{k} x_d^k (1 - x_d)^{6-k}, \quad k = 0 \ldots 6, \tag{1}$$

where $x_d = c_d/(c_d + c_a)$ is the molar fraction of I_d, and c_d and c_a are the molar concentrations of I_d and I_a, respectively. The binomial coefficient equals the number of possible permutations among the six insulin molecules forming a hexamer with k donors. Thus, each of the seven classes can be subdivided into $\binom{6}{k}$ permutations π_k, which results in a total number of 64 different hexamer types (Table 2). The energy transfer from the lth donor to any individual

TABLE 1 Distances between the N_ϵ atoms of the Lys^{B29} in the 2Zn insulin hexamer derived from the crystal coordinates: PDB 4INS (Baker et al., 1988).

Positions	Distance (Å)
1–2 = 2–3 = 3–1	34.4
1–4 = 2–5 = 3–6	31.5
1–5 = 2–6 = 3–4	43.5
1–6 = 2–4 = 3–5	50.5

The numbering refers to Fig. 1 *B*.

TABLE 2 Binomial subunit distribution over the hexamers for equimolar mixtures of donor (I_d) and acceptor insulin (I_a)

| | | | T | | Frequency of D-A separation | | | | | | | | | | | | | | | | | | | |
D:A	π	No.	$\{^{123}_{456}\}$	ν_T	1–2	1–4	1–5	1–6	1–2	1–4	1–5	1–6	1–2	1–4	1–5	1–6	1–2	1–4	1–5	1–6	1–2	1–4	1–5	1–6
0:6	1	1	$\{^{AAA}_{AAA}\}$	1	—	—	—	—	—	—	—	—	—	—	—	—	—	—	—	—	—	—	—	—
1:5	6	2	$\{^{DAA}_{AAA}\}$	6	2	1	1	1	—	—	—	—	—	—	—	—	—	—	—	—	—	—	—	—
2:4	15	3	$\{^{DDA}_{AAA}\}$	6	1	1	1	1	1	1	1	1	—	—	—	—	—	—	—	—	—	—	—	—
		4	$\{^{DAA}_{DAA}\}$	3	2	0	1	1	2	0	1	1	—	—	—	—	—	—	—	—	—	—	—	—
		5	$\{^{DAA}_{ADA}\}$	3	2	1	0	1	2	1	0	1	—	—	—	—	—	—	—	—	—	—	—	—
		6	$\{^{DAA}_{AAD}\}$	3	2	1	1	0	2	1	1	0	—	—	—	—	—	—	—	—	—	—	—	—
3:3	20	7	$\{^{DDD}_{AAA}\}$	2	0	1	1	1	0	1	1	1	0	1	1	1	—	—	—	—	—	—	—	—
		8	$\{^{DDA}_{DAA}\}$	6	1	0	1	1	1	1	1	0	2	0	1	0	—	—	—	—	—	—	—	—
		9	$\{^{DDA}_{ADA}\}$	6	1	1	0	1	1	0	1	1	2	0	0	1	—	—	—	—	—	—	—	—
		10	$\{^{DDA}_{AAD}\}$	6	1	1	1	0	1	1	0	1	2	1	0	0	—	—	—	—	—	—	—	—
4:2	15	11	$\{^{DDD}_{DAA}\}$	6	0	0	1	1	0	1	1	0	0	1	0	1	2	0	0	0	—	—	—	—
		12	$\{^{DDA}_{DDA}\}$	3	1	0	0	1	1	0	1	0	1	0	1	0	1	0	0	1	—	—	—	—
		13	$\{^{DDA}_{ADD}\}$	3	1	1	0	0	1	0	0	1	1	0	0	1	1	1	0	0	—	—	—	—
		14	$\{^{DDA}_{DAD}\}$	3	1	0	1	0	1	1	0	0	1	0	1	0	1	1	0	0	—	—	—	—
5:1	6	15	$\{^{DDD}_{DDA}\}$	6	0	0	0	1	0	0	1	0	0	1	0	0	1	0	0	0	1	0	0	0
6:0	1	16	$\{^{DDD}_{DDD}\}$	1	—	—	—	—	—	—	—	—	—	—	—	—	—	—	—	—	—	—	—	—

T, hexamer type, defined by a specific energy transfer distances pattern. No., running number of distance pattern. D:A, ratio of I_d and I_a in the hexamer. π, number of permutations for a given D:A ratio. ν_T, degeneracy of T, i.e., number of permutations with the same distance pattern. Permutations not explicitly listed are generated according to the following rules: $\{^{123}_{456}\} \Leftrightarrow \{^{465}_{132}\}$ and $\{^{123}_{456}\} \Leftrightarrow \{^{231}_{564}\}$.

acceptors in the permutation π_k is

$$E_l^{\pi_k} = \frac{\sum_a r_{da}^{-6}}{\mathbf{R}_0^{-6} + \sum_a r_{da}^{-6}}, \quad l = 1 \ldots k, \tag{2}$$

where $\mathbf{R}_0$ denotes the Förster distance characteristic of the specific donor-acceptor pair, and r_{da} is the distance between the donor l and an acceptor in the permutation π_k. Considering the energy transfer from several donors to several acceptors as independent events (Schulzki et al., 1990), the average energy transfer per donor of the permutation π_k is given by

$$\langle E^{\pi_k} \rangle = \frac{1}{k} \sum_{l=1}^{k} E_l^{\pi_k}.$$

Because each contribution to the sum depends solely on the distances between donors and acceptors, only those types among the permutations π_k have to be distinguished that show a different pattern of distances. This reduces the number of hexamer types from 64 to only 16 (see Table 2). The specific average energy transfer per donor for each of these types T is equal to

$$\langle E^T \rangle = \frac{1}{k_T} \sum_{l=1}^{k_T} E_l^T, \quad T = 1, \ldots, 16, \tag{3}$$

where k_T denotes the number of donors in type T. Each type occurs with a certain frequency ν_T (Table 2). The sum of ν_T over all types with the same number of donors k yields the binomial coefficient $\binom{6}{k}$. Hence, the probability for each of the 16 distinguishable hexamer types is

$$P_T = \nu_T x_d^{k_T} (1 - x_d)^{6-k_T}, \quad T = 1, \ldots, 16. \tag{4}$$

The mean energy transfer per donor in the mixture corresponds to the sum over all types T, each contributing a characteristic hexamer-average energy transfer $\langle E^T \rangle$ per donor. This summation has to be weighted by the number of donors contained in the respective hexamer type T, and additionally by the probability of its occurrence P_T. Finally, the sum has to be normalized by the mean number of donors in all types to obtain the mean energy transfer per donor of the mixture:

$$\langle E \rangle = \frac{\sum_{T=1}^{16} k_T P_T \langle E^T \rangle}{\sum_{T=1}^{16} k_T P_T} = \frac{\sum_{T=1}^{16} P_T \sum_{l=1}^{k_T} E_l^T}{\sum_{T=1}^{16} k_T P_T}. \tag{5}$$

The second equality follows because of Eq. 3. $\langle E \rangle$ in Eq. 5 can be equated to the total energy transfer of the mixture if the amount of oligomers other than hexamers is negligible, which can be achieved by sufficiently high total insulin concentration.

The kinetics of subunit interchange between insulin hexamers

Equimolar solutions of hexamers of N_ϵ^{B29}-Abz-insulin (donor insulin, I_d) and N_ϵ^{B29}-Tyr(NO$_2$)-insulin (acceptor insulin, I_a) were prepared at concentrations ≥ 1 g/l with 0.33 eq. divalent metal ions/monomer. The conformational state of the hexamers under these conditions is T_6. When equal volumes of these solutions are mixed, the total insulin concentration does not change. The fluorescence emission, however, decreases with time. The decrease is caused by the energy transfer that occurs as the subunits of hexamers interchange and hybrid hexamers are formed in a process that is entropy driven. A representative time course is shown in Fig. 2.
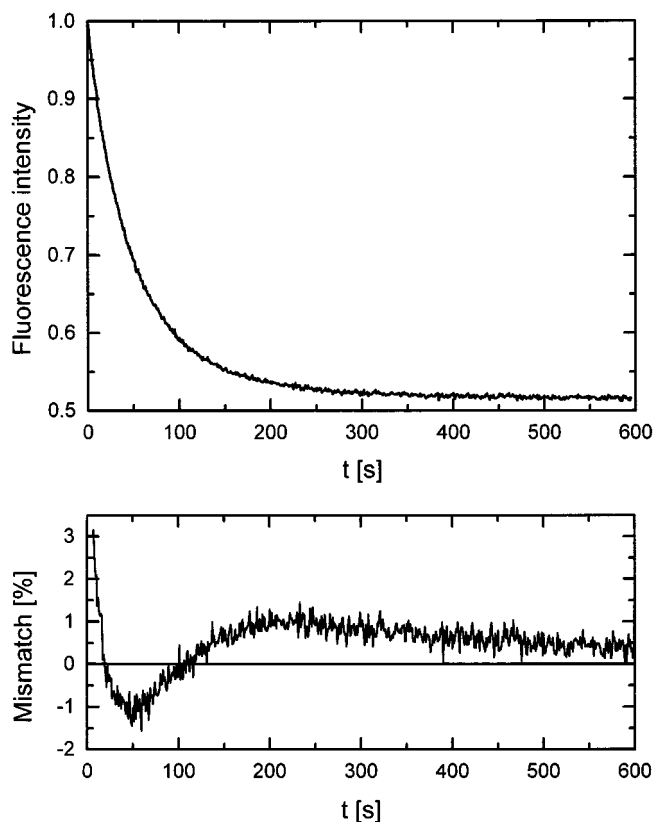
FIGURE 2 (*Top*) Representative time course of the normalized fluorescence intensity observable with mixing of equal volumes of equimolar solutions of donor and acceptor insulin. $c = 900$ μM; 0.33 equivalents Zn^{2+}/monomer; pH 7.8, without Tris. (*Bottom*) Residual mismatch of a least-squares fit by a single-exponential function.

As a first approximation, the curve was fitted with a single exponential function that proved quite acceptable according to the residuals included in Fig. 2.

The influence of concentration on the interchange kinetics

To learn about the order of the reaction, the interchange kinetics were measured as a function of the total insulin concentration. According to Table 3, the interchange rate increases with increasing concentration, indicating that the reaction is of higher than first order. Therefore, an isolated dissociation step, such as the dissociation of hexamers into

TABLE 3 Kinetic data on the subunit interchange as a function of the total insulin concentration

Concentration of insulin (μM)	$1/k_{app}$ (s)	R_0 (Å)	τ_{dim} (s)
180	147	30.1	75.0
540	105	30.9	47.5
1440	50	31.8	25.1

k_{app}, rate constant obtained by monoexponential fit. R_0, Förster distance derived from the total fluorescence change. τ_{dim}, hexamer lifetime. 0.33 equivalents Zn^{2+}/monomer; pH 7.8, without Tris; temperature: 20°C.

subunits, cannot be rate limiting. It could be, however, within a complex mechanism, if preceded by an association step, e.g., formation of a transition state.

The influence of temperature on the interchange kinetics

The interchange kinetics were measured at seven different temperatures, and the activation energy was derived from an Arrhenius plot of the rate constants over 1/T (Fig. 3) to be 90.4 kJ/mol. This value is comparable to the value for the hybridization of tetrameric glyceraldehyde 3-phosphate dehydrogenase (84 kJ/mol; Osborne and Hollaway, 1974) and of pig heart lactate dehydrogenase (83.7 kJ/mol; Erijman and Weber, 1993). It is significantly higher than the activation energies for the association and dissociation of the insulin dimer, 10.5 kJ/mol and 31 kJ/mol, respectively (Koren and Hammes, 1976). The order of magnitude of the rate constants and the value of the activation energy show that the subunit interchange is not controlled by diffusion (Levine, 1995).

Analysis of the time-dependent energy transfer approaching the steady state

The following analysis refers to conditions that are determined by inherent properties common to I_d and I_a and native insulin or are established experimentally. The latter conditions are the presence of metal ions and absolute concentrations high enough for essentially all insulin to exist in the hexameric state, i.e., the concentrations of subunits to be negligible with respect to energy transfer, but not zero (see below). The solutions of I_d and I_a mixed are of equal volume and concentration (symmetrical initial conditions). Owing to the fact that the presence of the labels does not interfere
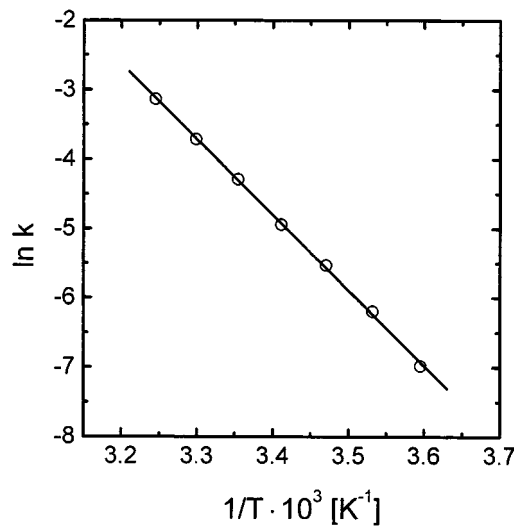

FIGURE 3 Temperature dependence of the subunit interchange reaction in the range 5–40°C: Arrhenius plot with the rate constants from monoexponential fit.

with the association/dissociation behavior (Hassiepen et al., 1998), the total concentrations of hexamers, tetramers, dimers, and monomers are constant. Furthermore, the equilibrium relating at least monomers and dimers is attained quasi-instantaneously. The rate constant of dimer dissociation k_- is inaccessible by stopped-flow methods. A value $k_- = 1.55 \times 10^4 \text{ s}^{-1}$ has been obtained by T-jump experiments (Koren and Hammes, 1976). The corresponding half-life period of the dimers $t_{1/2} = 4.5 \times 10^{-5}$ s is many orders of magnitude shorter than the time the interchange process is taking here. This extreme gap between the time scales, taken together with the symmetrical initial conditions, leads to the following statements, which greatly facilitate the analysis or even make it possible. With $[D]$, $[A]$ denoting the concentrations of donor and acceptor monomers, respectively, and $[DD]$, $[DA]$, and $[AA]$ denoting the concentrations of dimers composed correspondingly,

$$[D] = [A] = 1/2([D] + [A]) = \text{const.}, \quad (6)$$

$$[DD] = [AA] \approx 1/4([DD] + [DA] + [AA]) = \text{const.}$$
$$(7)$$
$$[DA] \approx 1/2([DD] + [DA] + [AA]) = \text{const.}$$

The derivation of these equations, as well as the limit of validity for the approximate equalities in Eq. 7, is given in Appendix A. It is convenient to introduce the relative concentrations of donor and acceptor monomers $x_D = [D]/([D] + [A])$, $x_A = [A]/([D] + [A]) = [A]/c_M$, respectively, and correspondingly, those for the dimers defined by $x_{DD} = [DD]/([DD] + [DA] + [AA])$, $x_{DA} = [DA]/([DD] + [DA] + [AA])$, $x_{AA} = [AA]/([DD] + [DA] + [AA]) = [AA]/c_D$. In terms of the relative concentrations, Eqs. 6 and 7 translate into
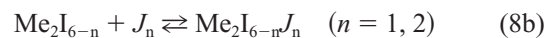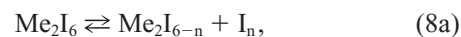
$$x_D = x_A = \tfrac{1}{2}, \quad (6a)$$

$$x_{DD} = x_{AA} \approx \tfrac{1}{4} \quad \text{and} \quad x_{DA} \approx \tfrac{1}{2}. \quad (7a)$$

The quantitative description of the kinetics of the subunit interchange between insulin hexamers requires a model. Any model mechanism has to comply with two observations: 1) increase in the interchange rate with total concentration, and 2) statistical distribution of I_d and I_a in the steady state. Furthermore, any model has to specify the molecular species that is actually exchanged. The exchange process is, of course, closely related to the association/dissociation processes for the hexamer. Whereas metal-bound tetramers seem to be accepted intermediates in hexamer formation (Coffman and Dunn, 1988), it is much less clear whether the hexamer is completed by cooperative binding of two monomers or by binding of a dimer. This would be the "natural" dimer, i.e., the one characterized by the antiparallel β-pleated sheet formed by the C-terminal B chains of the constituent monomers about the noncrystallographic *OP* axis (Blundell et al., 1972; dimer 1–4 = 2–5 = 3–6 in Fig. 1 *B*). Completion of the hexamer by the last dimer corresponds to the insertion of a keystone, which not
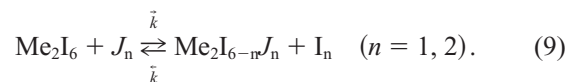
only engages two times two monomer/monomer contacts about the *OQ* axes at the same time (1 with 2 and 3 + 4 with 5 and 6, etc.; see Fig. 1 *B*), but also provides the two histidines lacking for complete metal coordination.

If the tetramer binds a monomer, the keystone effect is limited to one trimer by two monomer/monomer contacts and completion of the coordination of one metal. The true keystone in that case would be the last monomer with the same interactions as the former, but additionally one strong *OP* contact.

These considerations suggest either monomers or dimers to be the species actually exchanged, without implying any specific exchange mechanism. The subunit interchange could be imagined to proceed along either of the two following schemes:

$$\text{Me}_2\text{I}_6 \rightleftarrows \text{Me}_2\text{I}_{6-n} + \text{I}_n, \quad (8a)$$

$$\text{Me}_2\text{I}_{6-n} + J_n \rightleftarrows \text{Me}_2\text{I}_{6-n}J_n \quad (n = 1, 2) \quad (8b)$$

or

$$\text{Me}_2\text{I}_6 + J_n \overset{\vec{k}}{\underset{\bar{k}}{\rightleftarrows}} \text{Me}_2\text{I}_{6-n}J_n + \text{I}_n \quad (n = 1, 2). \quad (9)$$

Scheme 8 postulates that a hexamer first releases a subunit, either a monomer ($n = 1$) or a dimer ($n = 2$), before another corresponding subunit is reintegrated. This is analogous to the SN1 mechanism, the rate of which, however, is independent of concentration. Because of the concentration dependence observed for the present kinetics, scheme 8 can be ruled out. The scheme to be treated in greater detail thus is 9. This scheme is analogous to the SN2 mechanism, where the rate depends on the concentration of the "nucleophile," a role adopted here by the exchanging subunit. Scheme 9 will be elaborated below in the form of two models, one with the monomer ($n = 1$), the other with the dimer ($n = 2$), as the species that is actually exchanged in a simple bimolecular step. In the dimer model the compulsory involvement of monomers is fulfilled by coupling to the quasi-instantaneous monomer/dimer equilibration:

$$\text{I}_2 \leftrightarrow 2\text{I}; \quad \text{IJ} \leftrightarrow \text{I} + J; \quad J_2 \leftrightarrow 2J. \quad (9a)$$
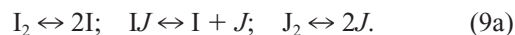
In Eq. 9 the rates and, hence, the rate constants for the forward and backward reactions are the same, i.e., $k_{\text{mon}} = \vec{k}_{\text{mon}} = \bar{k}_{\text{mon}}$ ($n = 1$); $k_{\text{dim}} = \vec{k}_{\text{dim}} = \bar{k}_{\text{dim}}$ ($n = 2$), because it is assumed that all striking and expelled subunits behave identically. The progress of the interchange reflected by the decrease in fluorescence emission results from the concentration change of the 16 hexamer types.

It will now be shown that the rate equations corresponding to the monomer and the dimer model (see scheme 9) can be formulated in terms of the lifetime of hexamers. The number of interchange processes per second is equal to the respective exchange rate, which is the product of either k_{mon} or k_{dim} and the concentration of the exchanging subunit species, i.e., either monomers or dimers. Therefore, the lifetime of hexamers for the respective model is given by its

reciprocal value:

$$\tau_{mon} = \frac{1}{k_{mon}([A] + [D])} = \frac{1}{k_{mon} \cdot c_M}, \quad (10a)$$

$$\tau_{dim} = \frac{1}{k_{dim}([AA] + [DD] + [DA])} = \frac{1}{k_{dim} \cdot c_D}. \quad (10b)$$

These relations allow us to formulate the rate equations for the elementary reactions (scheme 9) in terms of the respective lifetime, τ_{mon} or τ_{dim}. The column vector $\underline{H}$ can be introduced. $\underline{H}$ has the components $H_1, \ldots, H_{16}$, which denote the concentrations of the 16 spectroscopically distinguishable hexamer types. Now, the 16 rate equations can be written in matrix form:

$$\underline{\dot{H}} = k_{mon}\underline{\underline{M}}_{mon}([A], [D]) \cdot \underline{H} = \tau_{mon}^{-1} \underline{\underline{M}}_{mon}(x_A, x_D) \cdot \underline{H}, \quad (11a)$$

$$\underline{\dot{H}} = k_{dim}\underline{\underline{M}}_{dim}([AA], [DD], [DA]) \cdot \underline{H}$$
$$= \tau_{dim}^{-1} \underline{\underline{M}}_{dim}(x_{AA}, x_{DD}, x_{DA}) \cdot \underline{H}. \quad (11b)$$

To obtain the second equalities in Eqs. 11a and 11b, use can be made of the fact that the matrices $\underline{\underline{M}}$ are simply proportional to the concentrations of the exchanging subunit species, be they monomers or dimers. Therefore, the matrices $\underline{\underline{M}}$ can be rewritten in terms of the above introduced relative concentrations, x_A, x_D, and x_{AA}, x_{DD}, and x_{DA} (see above) multiplied by the total monomer, c_M, or dimer concentration, c_D.

The solutions of Eqs. 11a and 11b are the 16 different time-dependent hexamer concentrations, $\underline{H}(t; \tau)$. The hexamer concentrations further depend parametrically on the respective hexamer lifetime, either τ_{mon} or τ_{dim}. When a solution of Eqs. 11a and 11b has been obtained, the time-dependent probability of finding a hexamer of type T ($T = 1, \ldots, 16$) among all of the hexamers is given by $P_T(t) = H_T(t; \tau)/\Sigma_T H_T$, and the time-dependent overall energy transfer per donor in the mixture is obtained in a manner similar to that of Eq. 5 for the steady state:

$$\langle E \rangle(t) = \frac{\sum_{T=1}^{16} P_T(t)\langle E^T \rangle k_T}{\sum_{T=1}^{16} P_T(t) k_T} = \frac{\sum_{T=1}^{16} H_T(t; \tau)\langle E^T \rangle k_T}{\sum_{T=1}^{16} H_T(t; \tau) k_T}. \quad (12)$$

Once the functional form of $\underline{H}(t; \tau)$ is established, the lifetime of hexamers can be determined by varying it until the fit of $\langle E \rangle(t)$ in Eq. 12 to the experimental kinetics is optimum.

According to Eqs. 6a and 7a the matrices $\underline{\underline{M}}_{mon}$ and $\underline{\underline{M}}_{dim}$ in Eqs. 11a,b are constant, and the problem of determining the time-dependent energy transfer reduces to the standard task of solving a set of first-order differential equations with constant coefficients, given initial conditions $H_1(0) = H_{16}(0) = c_H/2$; $H_2(0) = \cdots = H_{15}(0) = 0$, where c_H is the total hexamer concentration.

The rate equations for the sixteen hexamer types

So far nothing has been said about the explicit construction of the elements of the matrices $\underline{\underline{M}}$ in Eqs. 11a and 11b. The matrix elements have to be obtained from the rate equations for the 16 hexamer types. Here only a few typical examples for the rate equations are discussed. The complete matrices $\underline{\underline{M}}$ corresponding to the rate equations of all 16 hexamer types can be found in Appendix B.

The monomer model is considered first. In terms of the lifetime of hexamers τ_{mon} and the relative concentrations $x_A = [A]/([A] + [D])$ and $x_D = [D]/([A] + [D])$, the rate equation for, e.g., hexamer type 4 reads

$$\dot{H}_4 = \tau_{mon}^{-1}\left\{ +\frac{1}{6} x_D H_2 + \left[-(x_A + x_D) + \frac{2}{3} x_A + \frac{1}{3} x_D \right] H_4 + \frac{1}{6} x_A H_8 + \frac{1}{6} x_A H_9 \right\}. \quad (13)$$

The factors in front of x_A and x_D can be understood as follows. In a representation of, for instance, hexamer type 4 by $\{^{DAA}_{DAA}\}$ (compare Table 2), the two rows represent the two trimers 1–3 and 4–6 (compare Fig. 1 B). Now if a donor monomer with the relative concentration x_D collides with a hexamer of type 2 $\{^{DAA}_{AAA}\}$, it will replace the first acceptor monomer in the lower trimer only in one-sixth of all cases. Consequently, only in one-sixth of all cases is the result a type 4 hexamer. If it replaces any other monomer, a different type of hexamer is formed. The term with the negative sign in Eq. 13 accounts for the fact that any collision of a type 4 hexamer with monomers will annihilate it and create a different type of hexamer with the following exceptions. If the striking monomer is an acceptor monomer, the resulting hexamer will still be of type 4 in two-thirds of all cases. Similarly, if the striking monomer is a donor monomer, the hexamer type 4 is reproduced in one-third of all cases. This is accounted for by the terms $+((2/3)x_A + (1/3)x_D)H_4$ in Eq. 13. The other two production terms describe the collisions of an acceptor monomer with a hexamer of type 8 $\{^{DDA}_{DAA}\}$ and of type 9 $\{^{DDA}_{ADA}\}$, respectively. In either case, a type 4 hexamer is produced only with a probability of 1/3. No other exchange processes are possible that could result in a hexamer of type 4. Therefore, the only nonvanishing matrix elements in the fourth row of $\underline{\underline{M}}_{mon}$ are

$$M_{4,2} = \frac{1}{6} x_D = \frac{1}{12}, \quad M_{4,4} = \frac{1}{3} x_D + \frac{2}{3} x_A - (x_A + x_D) = \frac{1}{2},$$

$$M_{4,8} = M_{4,9} = \frac{1}{6} x_A = \frac{1}{12}, \quad (14)$$

where $x_A = x_D = 1/2$ has been inserted (see Eq. 6a). On the basis of similar considerations, all other matrix elements for the monomer model can be constructed.

Before discussing two typical cases corresponding to the dimer model, it has to be noted that the replacement of a dimer in a hexamer $\{^{123}_{456}\}$ either concerns positions $^1_4$ or $^2_5$ or

$\frac{3}{6}$. The simplest possible example is the rate equation for hexamer type 1 $\{^{AAA}_{AAA}\}$:

$$\dot{H}_1 = \tau_{\text{dim}}^{-1}\left\{[-(x_{\text{AA}} + x_{\text{DD}} + x_{\text{DA}}) + x_{\text{AA}}]H_1 + \frac{1}{3}x_{\text{AA}}H_2\right.$$

$$\left. + \frac{1}{3}x_{\text{A}}H_4\right\}. \quad (15)$$

The first term with the negative sign indicates that whenever any dimer and a hexamer of type 1 collide, a new hexamer is produced. However, if the striking dimer is an acceptor homodimer, a type 1 hexamer is reproduced. This is described by the term $+x_{\text{AA}}H_1$. Type 1 hexamers can also be produced if acceptor homodimers collide with hexamers of type 2 $\{^{DAA}_{AAA}\}$, but only in one-third of all cases do the striking acceptor homodimers replace the heterodimer in hexamers of type 2. Correspondingly, a factor of 1/3 also applies to the exchange process with hexamers of type 4 $\{^{DAA}_{DAA}\}$. Exchange processes with other hexamers cannot result in hexamers of type 1. Thus, apart from zero entries, the first row of the matrix $\underline{M}_{\text{dim}}$ contains

$$M_{1,1} = (x_{\text{AA}} + x_{\text{DD}} + x_{\text{DA}}) - x_{\text{AA}} = \frac{3}{4},$$

$$M_{1,2} = \frac{1}{3}x_{\text{AA}} = \frac{1}{12}, \quad M_{1,4} = \frac{1}{3}x_{\text{AA}} = \frac{1}{12}, \quad (16)$$

where $x_{\text{DD}} = 1/4$, $x_{\text{DA}} = 1/2$, and $x_{\text{AA}} = 1/4$ has been inserted, which is approximately valid (compare Eq. 7b).

Another typical example is the one for hexamer type 3 $\{^{DDA}_{AAA}\}$:

$$\dot{H}_3 = \tau_{\text{dim}}^{-1}\left\{+\frac{1}{3}x_{\text{DA}}H_2 + [-(x_{\text{AA}} + x_{\text{DD}} + x_{\text{DA}})\right.$$

$$+ \frac{1}{3}x_{\text{DA}}H_3 + \frac{1}{3}x_{\text{DA}}H_5 + \frac{1}{3}x_{\text{DA}}H_6$$

$$+ x_{\text{AA}}H_7 + \frac{1}{6}x_{\text{DA}}H_8 + \frac{1}{6}x_{\text{DA}}H_9 + \frac{1}{3}x_{\text{AA}}H_{10}$$

$$+ \frac{1}{3}x_{\text{AA}}H_{11}. \quad (17)$$

Again, $-\tau_{\text{dim}}^{-1}(x_{\text{AA}} + x_{\text{DD}} + x_{\text{DA}})H_3$ are the annihilation terms, but the production terms are a bit more complicated as before. To formulate them correctly, it is necessary to take the relative orientation of the colliding species into account. If, for instance, a hexamer of type 2 $\{^{DAA}_{AAA}\}$ and a heterodimer collide to form a type 3 hexamer, the dimer must replace one of the two acceptor homodimers in hexamer type 2. The chance that this happens is 2/3.

Furthermore, the dimer must be incorporated with the appropriate orientation, so that the two donor subunits are in the same trimer. This halves the chance for production of type 3 hexamers, and, consequently, a factor of 1/3 appears in front of $x_{\text{DA}}H_2$. The other terms in Eq. 17 can be

constructed analogously, and the matrix elements are obtained as before, setting $x_{\text{AA}} = 1/4$, $x_{\text{DD}} = 1/4$, and $x_{\text{DA}} = 1/2$.

To check whether the matrix elements are correctly constructed, use can be made of the fact that the equilibrium distribution predicted by Eq. 4 must be a fixed point of the rate equations. More precisely, denoting the equilibrium concentrations by $H_T(t \to \infty) = H_T^{\text{eq}} = P_T c_H$, $T = 1, \ldots,$ 16, where P_T denotes the equilibrium probability of hexamer type T in Eq. 4, the equilibrium concentrations H_T^{eq} must be solutions of the 16 equations $\dot{H}_i^{\text{eq}} \equiv 0 = \Sigma_{T=1}^{16} M_{i,T}H_T^{\text{eq}}$, $i = 1, \ldots, 16$. Another check is to sum up the elements in each column of the matrix $\underline{M}$. These must add to zero because the total hexamer concentration is constant. Because this must hold for an arbitrary distribution of the hexamer types, the 16 conditions $\Sigma_{i=1}^{16} M_{i,j} = 0$, $j = 1, \ldots,$ 16 are obtained. A third criterion for the correctness of the matrices concerns the stability of the solutions of Eq. 11a and 11b. To represent stable solutions, all nonvanishing (real) eigenvalues of the matrices need to be negative. These three checks were performed, and the criteria were found to be fulfilled for both matrices $\underline{M}_{\text{mon}}$ and $\underline{M}_{\text{dim}}$.

The systems of first-order differential equations with constant coefficients (Eqs. 11a and 11b) were solved with the computer algebra program MAPLE. Inserting these solutions into Eq. 12 finally yields the following expressions for the time-dependent energy transfer per donor. For the monomer model:

$$\langle E\rangle(t) = \frac{1}{3}\left\{A_{\text{mon}} + B_{\text{mon}}\exp\left(-\frac{t}{\tau_{\text{mon}}}\right) + C_{\text{mon}}\exp\left(-\frac{2t}{3\tau_{\text{mon}}}\right)\right.$$

$$\left. + D_{\text{mon}}\exp\left(-\frac{t}{3\tau_{\text{mon}}}\right)\right\}, \quad (18a)$$

where the coefficients $A_{\text{mon}} \cdots D_{\text{mon}}$ are given as combinations of the products $\langle Q^T\rangle \equiv \langle E^T\rangle k_T$, $(T = 1, \ldots, 16)$, which are quantities specific for the 16 different hexamer types (compare Eqs. 5 and 12). Because the energy transfer in hexamers of type 1 and of type 16 is zero ($\langle Q^1\rangle = \langle Q^{16}\rangle = 0$), the coefficients $A_{\text{mon}} \cdots D_{\text{mon}}$ depend only on $\langle Q^2\rangle \ldots \langle Q^{15}\rangle$:

$$A_{\text{mon}} = \frac{1}{64}\{6\langle Q^2\rangle + 6\langle Q^3\rangle + 3\langle Q^4\rangle + 3\langle Q^5\rangle + 3\langle Q^6\rangle$$

$$+ 2\langle Q^7\rangle + 6\langle Q^8\rangle + 6\langle Q^9\rangle + 6\langle Q^{10}\rangle + 6\langle Q^{11}\rangle$$

$$+ 3\langle Q^{12}\rangle + 3\langle Q^{13}\rangle + 3\langle Q^{14}\rangle + 6\langle Q^{15}\rangle\},$$

$$B_{\text{mon}} = \frac{1}{64}\{-6\langle Q^2\rangle + 6\langle Q^3\rangle + 3\langle Q^4\rangle + 3\langle Q^5\rangle + 3\langle Q^6\rangle$$

$$- 2\langle Q^7\rangle - 6\langle Q^8\rangle - 6\langle Q^9\rangle - 6\langle Q^{10}\rangle + 6\langle Q^{11}\rangle$$

$$+ 3\langle Q^{12}\rangle + 3\langle Q^{13}\rangle + 3\langle Q^{14}\rangle - 6\langle Q^{15}\rangle\},$$

$$C_{\text{mon}} = \frac{1}{64}\{-30\langle Q^2\rangle - 6\langle Q^3\rangle - 3\langle Q^4\rangle - 3\langle Q^5\rangle - 3\langle Q^6\rangle$$

$$+ 6\langle Q^7\rangle + 18\langle Q^8\rangle + 18\langle Q^9\rangle + 18\langle Q^{10}\rangle$$

$$- 6\langle Q^{11}\rangle - 3\langle Q^{12}\rangle - 3\langle Q^{13}\rangle - 3\langle Q^{14}\rangle$$

$$- 30\langle Q^{15}\rangle\},$$

$$D_{\text{mon}} = \frac{1}{64}\{30\langle Q^2\rangle - 6\langle Q^3\rangle - 3\langle Q^4\rangle - 3\langle Q^5\rangle - 3\langle Q^6\rangle$$

$$- 6\langle Q^7\rangle - 18\langle Q^8\rangle - 18\langle Q^9\rangle - 18\langle Q^{10}\rangle$$

$$- 6\langle Q^{11}\rangle - 3\langle Q^{12}\rangle - 3\langle Q^{13}\rangle - 3\langle Q^{14}\rangle$$

$$+ 30\langle Q^{15}\rangle\}.$$

Similarly, for the dimer model,

$$\langle E\rangle(t) = \frac{1}{3}\left\{A_{\text{dim}} + B_{\text{dim}}\exp\left(-\frac{t}{\tau_{\text{dim}}}\right) + C_{\text{dim}}\exp\left(-\frac{2t}{3\tau_{\text{dim}}}\right)\right.$$

$$\left. + D_{\text{dim}}\exp\left(-\frac{t}{3\tau_{\text{dim}}}\right)\right\}, \quad (18b)$$

but with the different coefficients $B_{\text{dim}} \cdots D_{\text{dim}}$. A_{dim} equals A_{mon}, as it should:

$$B_{\text{dim}} = \frac{1}{64}\{-30\langle Q^2\rangle + 6\langle Q^3\rangle - 9\langle Q^4\rangle + 3\langle Q^5\rangle + 3\langle Q^6\rangle$$

$$- 2\langle Q^7\rangle + 18\langle Q^8\rangle + 18\langle Q^9\rangle - 6\langle Q^{10}\rangle + 6\langle Q^{11}\rangle$$

$$- 9\langle Q^{12}\rangle + 3\langle Q^{13}\rangle + 3\langle Q^{14}\rangle - 30\langle Q^{15}\rangle\},$$

$$C_{\text{dim}} = \frac{1}{64}\{18\langle Q^2\rangle - 6\langle Q^3\rangle - 3\langle Q^4\rangle - 3\langle Q^5\rangle - 3\langle Q^6\rangle$$

$$+ 6\langle Q^7\rangle - 30\langle Q^8\rangle - 30\langle Q^9\rangle + 18\langle Q^{10}\rangle - 6\langle Q^{11}\rangle$$

$$- 3\langle Q^{12}\rangle - 3\langle Q^{13}\rangle - 3\langle Q^{14}\rangle + 18\langle Q^{15}\rangle\},$$

$$D_{\text{dim}} = \frac{1}{64}\{6\langle Q^2\rangle - 6\langle Q^3\rangle + 9\langle Q^4\rangle - 3\langle Q^5\rangle - 3\langle Q^6\rangle$$

$$- 6\langle Q^7\rangle + 6\langle Q^8\rangle + 6\langle Q^9\rangle - 18\langle Q^{10}\rangle - 6\langle Q^{11}\rangle$$

$$+ 9\langle Q^{12}\rangle - 3\langle Q^{13}\rangle - 3\langle Q^{14}\rangle + 6\langle Q^{15}\rangle\}.$$

The two models predict the same equilibrium distribution among the 16 different hexamer types T, $T = 1, \ldots, 16$. The probabilities P_T of Eq. 5 can simply be read off from the expressions for $A_{\text{mon}} = A_{\text{dim}}$ as the factors in front of the quantities $\langle Q^T\rangle$, which are hexamer-type specific (except for type 1 and type 16, which do not contribute to the total energy transfer). The factor 1/3 in front of the curly brackets in Eqs. 18a and 18b reflects the normalization constant, $\Sigma_T P_T k_T = 3$ in Eq. 5, which is the mean number of fluorescence donors per hexamer, and which guarantees that $\langle E\rangle(t)$ represents the (time-dependent) mean energy transfer per donor.

As a further alternative to the monomer and dimer models, a tetramer model might be considered. In this case, corresponding to $n = 4$ in Eq. 9, 10 types of different D/A composition have to be taken into account, each representing a collision partner for any specific hexamer type. The kinetic analysis on the basis of the tetramer model was also feasible if the subunit interchange between tetramers was assumed to be quasi-instantaneous. As all interchange kinetics observed in the absence of metal ions are very rapid, this assumption might be justified. For the tetramer model only the final result is quoted (see Eq. 18c) without showing the complete matrices in an appendix:

$$\langle E(t)\rangle = \frac{1}{3}\left\{A_{\text{tet}} + B_{\text{tet}}\exp\left(-\frac{t}{\tau_{\text{tet}}}\right) + C_{\text{tet}}\exp\left(-\frac{2t}{3\tau_{\text{tet}}}\right)\right\},$$

$$(18c)$$

where $A_{\text{tet}} = A_{\text{dim}} = A_{\text{mon}}$, and the other two coefficients are given by

$$B_{\text{tet}} = \frac{1}{64}\{-12\langle Q^2\rangle - 12\langle Q^4\rangle + 4\langle Q^7\rangle - 12\langle Q^8\rangle$$

$$- 12\langle Q^9\rangle - 12\langle Q^{10}\rangle - 12\langle Q^{12}\rangle - 12\langle Q^{15}\rangle\},$$

$$C_{\text{tet}} = \frac{1}{64}\{-2\langle Q^2\rangle - 6\langle Q^3\rangle + 9\langle Q^4\rangle - 3\langle Q^5\rangle - 3\langle Q^6\rangle$$

$$- 6\langle Q^7\rangle + 6\langle Q^8\rangle + 6\langle Q^9\rangle - 18\langle Q^{10}\rangle - 6\langle Q^{11}\rangle$$

$$+ 9\langle Q^{12}\rangle - 3\langle Q^{13}\rangle - 3\langle Q^{14}\rangle + 6\langle Q^{15}\rangle\}.$$

In Eq. 18c τ_{tet} denotes the lifetime of hexamers if it is assumed that tetramers are the exchanging subunits. In analogy to Eqs. 10a,b, the lifetime τ_{tet} is given by $\tau_{\text{tet}} = 1/(k_{\text{tet}} \cdot c_{\text{tet}})$, where c_{tet} is the tetramer concentration and k_{tet} is the specific tetramer exchange rate.

The fitting procedure

There is still some uncertainty about the absolute values of the characteristic energy transfer per donor $\langle E^T\rangle$ of the single hexamer types T that determine the coefficients $A_{\text{mon,dim}}$, $B_{\text{mon,dim}}$, $C_{\text{mon,dim}}$, and $D_{\text{mon,dim}}$ in Eqs. 18a,b, respectively. This is the case because $\langle E^T\rangle$ depends on the distances between donors and acceptors, r_{da}, and the Förster distance $\mathbf{R}_0$ (compare Eqs. 2 and 3).

As for r_{da}, the distances are accessible by two approaches. They can be replaced by the distances between the ϵ-amino groups of the Lys[B29] in the x-ray structure that the labels are attached to. However, these are, of course, not identical to the distances between the transition centers of the label chromophores. Furthermore, the labels are subject to structural flexibility (Hassiepen et al., 1998). Separations of donors and acceptors can also be determined by energy transfer measurements if $\mathbf{R}_0$ is known. This possibility, however, exists for a single donor/acceptor pair, but not for a situation as complex as that in the insulin hexamer.

As for $\mathbf{R}_0$, the Förster distance is a constant characteristic of a specific donor-acceptor pair that can be determined experimentally, provided that information is available or reasonable assumptions can be made about the relative orientation of the labels' transition moments.

An adjustment had to be made for the total change in $\langle E \rangle(t)$ observed to equal $1/3 \, A_{mon,dim}$ in Eqs. 18a,b, respectively. As there is no reasonable basis for adjusting the multiple r_{da} values, it was decided pragmatically to continue using the distances between the N_ϵ^{B29} atoms in the x-ray structure and to achieve adjustment by variation of a single parameter only, $\mathbf{R}_0$. Thereupon $\langle E \rangle(t)$ in Eqs. 18a and 18b depends solely on the lifetime of the hexamers τ_{mon} and τ_{dim}, respectively. The lifetime could then be determined by reproducing the time course of the interchange by least-squares fit. The underlying $\mathbf{R}_0$ values are given together with the lifetimes obtained for the single experiments in Tables 3–5. They vary in the range $\pm 5\%$, with increasing $T \rightarrow R$ transformation, and are 4–14% higher than a value determined experimentally ($\mathbf{R}_0 = 28.9$ Å; Hassiepen et al., 1998).

Comparison of the models

A very acceptable fit of the experimental kinetics is already achieved with a single-exponential function, as shown by the residuals displayed in Fig. 2. There is a slight improvement of the fit based on the monomer and tetramer models (Eqs. 18a and c) and, notably, the dimer model (Eq. 18b) (compare Fig. 4). (The residuals for the tetramer model are similar to those of the monomer model and are not shown.) The performance of the model descriptions is reflected by the numerical values that the coefficients B, C, and D of the exponential functions in Eqs. 18a–c adopt. For the kinetics shown in Fig. 2 these are:

$$B_{mon} = -0.0006, \quad C_{mon} = -0.1287, \quad D_{mon} = -1.3902;$$

$$B_{dim} = -0.1077, \quad C_{dim} = -0.9984, \quad D_{dim} = -0.4134;$$

$$B_{tetr} = -1.1055, \quad C_{tetr} = -0.4134.$$

In the case of the monomer model, one of the exponential functions is prominent, owing to its coefficient (D_{mon}). Hence, it essentially corresponds to a monoexponential fit. With the dimer and tetramer models, substantial values are

obtained for two of the coefficients (C_{dim} and D_{dim} for the former and B_{tetr} and C_{tetr} for the latter).

Fitting either model to the experimental time courses, however, results in very similar values for the hexamer lifetime. It is therefore neither necessary nor really possible on the basis of the small difference in the quality of fit to prefer one model to the other.

However, dissociation of the hexamer will proceed as the reversal of its assembly and, hence, the most likely species that is exchanged seems to be the dimer. Therefore the dimer model was chosen for the following exemplary analyses of all experimental interchange kinetics. The relaxation times of the exponential functions in Eq. 18b depend solely on the lifetime of the hexamers. The latter is the reciprocal of a product of the interchange rate constant k_{dim} and the concentration of free dimers, c_D (see Eq. 10b). In the following it will be shown that all experimental influences on the interchange time course can be explained by changes in these factors.

The influence of metal ions on the interchange kinetics

The nature of the metal ions was varied at a constant stoichiometry of 0.33 Me^{2+}/insulin monomer. When the rate constants are ranked according to their magnitude as in Table 4, the order resulting for the metal ions is different from the order obtained upon ranking by their binding constants. Because not all binding constants of insulin for these ions are available, the constants included in Table 4 are those for the formation of their Tris-imidazole complexes (Sundberg and Martin, 1974). Comparison with imidazole seems reasonable because in the insulin hexamer each of the two metal ions is also coordinated by the imidazole groups of 3 His^{B10} side chains. The order of the metal ions ranked by their interchange rate constants is at variance with the order obtained for the constants of imidazole complex formation. Interestingly, however, it is the same as the order in a ranking of the metal ions according to the characteristic rate constants for H_2O substitution in their inner coordination sphere (see also Table 4). The enormous difference in the absolute values of the rate constants may be explained by the huge difference in the size and mobility of insulin on the one hand and water molecules

TABLE 4 Kinetic data on the subunit interchange between metal insulin hexamers, k_{app}, τ_{dim}; and on H_2O exchange in the inner coordination sphere of metal ions, k_{H_2O}; as well as logarithms of stability constants of the metal/imidazole complexes, K

Metal	$1/k_{app}$ (s)	$\mathbf{R}_0$ (Å)	τ_{dim} (s)	r	$1/k_{H_2O}$ (s)	r	log K/(M^{-1})	r
Cu^{2+}	1.43×10^2	26.5	7.69×10^1	1	5×10^{-9}	1	10.50	1
Zn^{2+}	2.08×10^2	29.1	1.09×10^2	2	5×10^{-8}	2	7.16	3
Co^{2+}	5.0×10^3	31.0	2.54×10^3	3	3.3×10^{-7}	3	5.75	4
Ni^{2+}	5.0×10^4	31.2	2.78×10^4	4	3.3×10^{-5}	4	7.50	2

k_{H_2O} values for Cu^{2+} and Zn^{2+}: Eigen (1963), for Co^{2+} and Ni^{2+}: Docummun and Merbach (1986). log $K = \Sigma_1^3 \log K_x$; $K_x = [(Me \cdot imidazole_x)^{2+}]/[(Me \cdot imidazole_{x-1})^{2+}] \cdot [imidazole]$ (Sundberg and Martin, 1974). For k_{app}, $\mathbf{R}_0$, and τ_{dim}, see Table 3. r, ranking according to the respective criterion. $c = 180$ μM; 0.33 equivalents divalent metal/monomer; pH 7.8, without Tris; temperature: 20°C.

TABLE 5 Kinetic data on the subunit interchange at different stages of ligand-induced T → R transformation

Eq. ligand/monomer			$1/k_{app}$ (s)	R_0 (Å)	τ_{dim} (s)	τ_{dim}
0	—	$\mathbf{T_6}$	1.47×10^2	30.1	7.5×10^1	1.25 min
8	Phenol	$\mathbf{T_3R_3}$	5.82×10^3	32.3	3.24×10^3	54.0 min
80	KSCN	$\mathbf{T_3R_3}$	5.55×10^3	32.7	3.31×10^3	58.2 min
10	Phenol	$\mathbf{T_3R_3}/\mathbf{R_6}$	9.44×10^3	32.5	5.35×10^3	1.49 h
15	Phenol	$\mathbf{T_3R_3}/\mathbf{R_6}$	2.33×10^4	32.8	1.35×10^4	3.75 h
20	Phenol	$T_3R_3/\mathbf{R_6}$	5.32×10^4	33.0	2.94×10^4	8.17 h

The predominant conformational state is indicated by bold letters. For k_{app}, R_0, and τ_{dim}, see Table 3. $c = 180$ μM; 0.33 equivalents Zn^{2+}/monomer; 25 mM Tris/HCl, pH 7.8; temperature: 20°C.

on the other. Insulin can thus be viewed in two different ways, either as a metal-binding protein or a metal ligand.

The influence of the conformational state of the hexamers on the interchange kinetics

Insulin hexamers can exist in essentially three different conformational states, T_6, T_3R_3, and R_6, all defined by x-ray crystallography (Baker et al., 1988; Bentley et al., 1976; Derewenda et al., 1989; Smith and Dodson, 1992). The main difference is that in T residues B1–B8 are in an extended conformation, whereas in R they are part of the central B-helix. Furthermore, the metal coordination in a T_3 trimer is octahedral, whereas in R_3 it is tetrahedral. In solution the three states are interrelated by dynamic equilibria. Normally extremely T-sided, the equilibria can be shifted R-ward by two completely different kinds of ligands, inorganic anions and phenolic compounds. The former, such as $SCN^{\ominus}$, are bound to one of the metal ions on the threefold axis, and the transformation cannot exceed the asymmetrical T_3R_3 state. Phenol binds to six specific sites at the subunit interfaces of each trimer. The hexamer behaves like a dimer of positively cooperative trimers related by negative cooperativity (Krüger et al., 1990). It is, therefore, possible to either establish the T_3R_3 state by an adequately moderate concentration of phenol or R_6 by an adequate excess of the ligand.

The T → R transformation increases the kinetic stability of the hexamers dramatically. The interchange kinetic data for different conformational states are listed in Table 5.
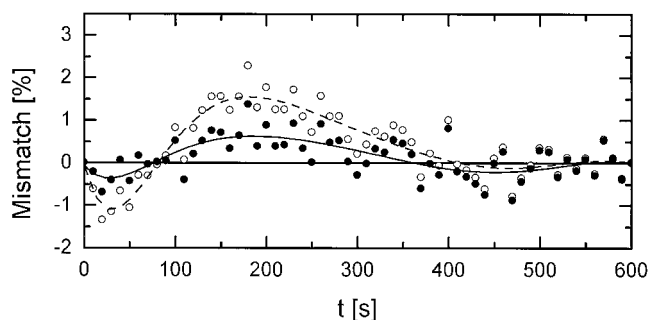
Their lifetime, only half a minute under T_6 conditions, is prolonged to 8 h at an excess of 20 moles phenol per monomer, when according to spectroscopic criteria the transformation appears to be about complete. It is important to note that for T_3R_3 τ_{dim} is essentially the same, whether this state is established with $SCN^{\ominus}$ ions or phenol as transforming ligands. As in the case of the metal ions, the influence of the ligands is mainly included in k_{dim}.

An increasingly high excess of phenol suppresses the subunit interchange reaction even further. At a molar ratio of 60, the lifetime is 3.4 days. According to scheme 9 this means that fewer and fewer subunits are available for the exchange reaction. Phenol not only promotes the T → R transformation, but is also known to enhance the assembly of hexamers (Bakaysa et al., 1996; Rahuel-Clermont et al., 1997). As the propensity of subunits to adopt the R state is extremely low, only a small fraction of the remaining subunits would count if adoption of the R state were the prerequisite for exchange with a R_6 hexamer in terms of scheme 9.

The lifetime of the hexamers is four to six orders of magnitude longer than that for bound phenol, which according to its NMR chemical shifts is less than 10 ms (Roy et al., 1989; Jacoby et al., 1996). Given that the ligand is almost completely buried in the hexamer (Derewenda et al., 1989),

FIGURE 4 Residual mismatch of fits of the subunit interchange kinetics in Fig. 2 on the basis of the monomer model (Eq. 18a, *open circles* and *broken line*) and the dimer model (Eq. 18b, *full circles* and *line*).
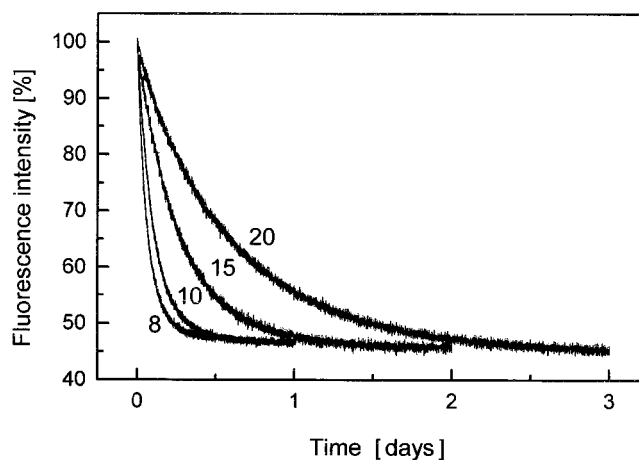

FIGURE 5 The subunit interchange kinetics at different stages of the T → R transformation of the hexamers achieved by increasing concentration of phenol. (Numbers indicate the equivalents phenol/monomer.) $c = 180$ μM; 0.33 equivalents Zn^{2+}/monomer; 25 mM Tris/HCl, pH 7.8.

it hence seems obvious that ligand binding and release do not require the hexamer to dissociate into subunits. Consequently, the ligand must enter and leave through a tunnel formed by fluctuations within the intact hexamer. Fluctuations of this kind are inferred from the rates of aromatic ring rotation and amide proton exchange in the R_6 hexamer. Many such rates are also much faster than subunit exchange. The fluctuations, however, seem insufficient to allow the access of water to the most stably bound protons. Their exchange will require dissociation of a subunit (Jacoby et al., 1996). The process of phenol binding and release and the tunnel used are currently being investigated by a special molecular dynamics simulation technique (Swegat, thesis in progress).

CONCLUSION

Insulin can be covalently labeled at Lys^{B29} with fluorescence donor and acceptor groups, respectively, without its tertiary structure or self-association being affected. Hexamers of donor and acceptor insulin were mixed, and the hybrid hexamers that formed were monitored by fluorescence energy transfer. By this approach the interchange of subunits between insulin hexamers was measured for the first time. The entropy-driven process relaxes to the statistical distribution of donor and acceptor insulin over 16 different types of hexamers, which is possible only if monomers are involved. The interchange kinetics were reproduced by model descriptions with monomers or dimers (or tetramers) as the species actually exchanged. The relaxation times figuring in the sum of exponential terms that describe the time-dependent energy transfer only depend on a single parameter, which is the lifetime of the hexamers. The lifetime is the reciprocal of the product of the concentration of the exchanged species and the rate constant. The latter includes all effects on the stability of the hexamers exerted by different metal ions or ligands for $T \rightarrow R$ conversion, for instance. The lifetime covers a range from half a minute for T_6 between 8 h and days for R_6 hexamers, depending on the excess of phenol. Although they are based on a simple bimolecular mechanism, the models used achieve a satisfactory reproduction of the experimental interchange kinetics.

APPENDIX A

In this appendix it is proved on the basis of the dimer model that whereas the insulin hexamers interchange their subunits, i.e., the concentrations of the 16 hexamer types vary, the five monomer and dimer concentrations [A], [D], [AA], [DD], and [DA] can be considered as constants.

This, however, has to be proved on the basis of the 21 coupled rate equations for monomers, dimers, and hexamers, and not by just using the five rate equations for an isolated monomer-dimer system. Nevertheless, the isolated monomer-dimer system is considered first because the general case of the 21 coupled rate equations for monomers, dimers, and hexamers can be treated as a perturbation of two systems of equations, which are five equations for the isolated monomer/dimer system and the 16 rate equations

for the hexamers and dimers. The isolated system of rate equations for the five dimer and monomer concentrations is analyzed first.

The monomer-dimer system in the absence of hexamers

Two equal volumes of pure donor insulin and pure acceptor insulin of equal concentration are combined at time $t = 0$. For a monomer/dimer system the five rate equations read

$$[\dot{AA}] = k_+[A]^2 - k_-[AA], \tag{A1}$$

$$[\dot{DD}] = k_+[D]^2 - k_-[DD], \tag{A2}$$

$$[\dot{DA}] = 2k_+[D] \cdot [A] - k_-[DA], \tag{A3}$$

$$[\dot{A}] = 2k_-[AA] + k_-[DA] - 2k_+[A]^2 - 2k_+[D] \cdot [A], \tag{A4}$$

$$[\dot{D}] = 2k_-[DD] + k_-[DA] - 2k_+[D]^2 - 2k_+[D] \cdot [A]. \tag{A5}$$

It should be noted that the statistical factor 2 in front of the product $[D] \cdot [A]$ in Eqs. A3–A5 accounts for the fact that heterodimers are twice as probable as either of the homodimers. For the above-mentioned initial conditions of equal concentrations and equal volumes of donor insulin and acceptor insulin, the rate equations can be solved without any approximations. Equations A1–A5 involve four constant functions of the concentrations. Two of them are the total monomer concentration $[A] + [D]$, and the total dimer concentration $[AA] + [DD] + [DA]$, because the total equilibrium between monomers and dimers is unperturbed by the mixing process. Because of the equivalence of donors and acceptors, the other two constants are $\delta \equiv [A] - [D] = 0$, and $\Delta \equiv [AA] - [DD] = 0$. Together, these are four constants formed by the five species in Eqs. A1–A5. There is only one free variable left that can be chosen to be the heterodimer concentration $[DA]$. The rate Eq. A3 for $[DA]$ can be reformulated using the above constants:

$$[\dot{DA}] = -k_-[DA] + \frac{k_+}{2}([A] + [D])^2. \tag{A6}$$

The solution of this equation corresponding to the initial condition $[DA](0) = 0$ reads

$$[DA](t) = \frac{K}{2}([A] + [D])^2(1 - \exp(-k_-t)), \tag{A7}$$

where $K = k_+/k_-$ denotes the equilibrium constant of association. The time dependence of the other four concentrations can be formulated as combinations of $[DA](t)$ and the four constants. However, in a kinetic experiment with fluorescence donors and acceptors distributed over monomers and dimers, only the heterodimer concentration $[DA](t)$ determines the time-dependent energy transfer: $\langle E \rangle(t) \propto [DA](t)$. Thus, Eq. A7 is promising because it directly relates the time course of the measured energy transfer to the dissociation rate k_- of dimers. Unfortunately, the monomer exchange in the dimers is too fast to be observable in stopped-flow experiments. A value of the rate constant for the dissociation of insulin dimers determined by T-jump methods is $k_- = 1.55 \times 10^4 \text{ s}^{-1}$ (Koren and Hammes, 1976). This justifies considering the monomer-dimer equilibration as an instantaneous process relative to the time scale on which the subunit interchange between hexamers occurs.

Uncoupling of the subunit interchange between dimers from that between hexamers

The simple solution (Eq. A7) of the rate equations of the previous section is no longer valid, because the elementary reactions (Eq. 9) do couple to the monomer-dimer equilibration process (Eq. 9a). However, if the perturbing influence of the coupling between the 16 rate equations and the five monomer/dimer equations is small, it can be expected that the time dependence of the dimer concentrations and thus of the matrix $\underline{M}_{\mathrm{dim}}(t)$ can be neglected on the time scale relevant for subunit interchange between hexamers. Because of the quasi-instantaneous equilibration between monomers and dimers, the time evolution for the dimer species would then effectively uncouple from the time evolution of the hexamers.

The rate equations for the five different monomer and dimer concentrations are reconsidered, but now for the presence of hexamers. In the case of the dimer model the two rate Eqs. A4 and A5 for the monomers in the presence of hexamers do not change, and only the three Eqs. A1–A3 for the dimer concentrations need to be rewritten:

$$[A\dot{A}] = -k_-[AA] + k_+[A]^2$$
$$- k_{\mathrm{dim}}\{[AA]c_{\mathrm{H}} - ([AA] + [DD] + [DA])j_{\mathrm{AA}}\}, \quad (A8)$$

$$[D\dot{D}] = -k_-[DD] + k_+[D]^2$$
$$- k_{\mathrm{dim}}\{[DD]c_{\mathrm{H}} - ([AA] + [DD] + [DA])j_{\mathrm{DD}}\}, \quad (A9)$$

$$[D\dot{A}] = -k_-[DA] + 2k_+[D][A]$$
$$- k_{\mathrm{dim}}\{[DA]c_{\mathrm{H}} - ([AA] + [DD] + [DA])j_{\mathrm{DA}}\}. \quad (A10)$$

They differ from Eqs. A1–A3 only by the additional terms $-k_{\mathrm{dim}}\{\ldots\}$. The first additional terms are annihilation velocities, $-k_{\mathrm{dim}} c_{\mathrm{H}}[AA]$ in Eq. A8, $-k_{\mathrm{dim}} c_{\mathrm{H}}[DD]$ in Eq. A9, and $-k_{\mathrm{dim}} c_{\mathrm{H}}[DA]$ in Eq. A10, where $c_{\mathrm{H}} = \Sigma H_{\mathrm{T}}$ denotes the total hexamer concentration. These terms describe the fact that a specific dimer is consumed by incorporation into a hexamer. Correspondingly, the production velocities $+ k_{\mathrm{dim}} ([AA] + [DD] + [DA])j$, where j stands for j_{AA}, j_{DD}, or j_{DA}, describe the appearance of one of the three dimer types by expellation from the hexamer. The terms j_{AA}, j_{DD}, and j_{DA} are abbreviations that stand for

$$j_{\mathrm{AA}} = H_1 + \frac{2}{3} H_2 + \frac{1}{3} H_3 + \frac{2}{3} H_4 + \frac{1}{3} H_5 + \frac{1}{3} H_6 + \frac{1}{3} H_8$$
$$+ \frac{1}{3} H_9 + \frac{1}{3} H_{12}, \quad (A11)$$

$$j_{\mathrm{DD}} = \frac{1}{3} H_4 + \frac{1}{3} H_8 + \frac{1}{3} H_9 + \frac{2}{3} H_{11} + \frac{1}{3} H_{12} + \frac{1}{3} H_{13}$$
$$+ \frac{1}{3} H_{14} + \frac{2}{3} H_{15} + H_{16}, \quad (A12)$$

$$j_{\mathrm{DA}} = \frac{1}{3} H_2 + \frac{2}{3} H_3 + \frac{2}{3} H_5 + \frac{2}{3} H_6 + H_7 + \frac{1}{3} H_8 + \frac{1}{3} H_9$$
$$+ H_{10} + \frac{2}{3} H_{11} + \frac{2}{3} H_{13} + \frac{2}{3} H_{14} + \frac{1}{3} H_{15}. \quad (A13)$$

The factors in front of the hexamer concentrations $H_1 \ldots H_{16}$ result from the fact that the different hexamer types are composed of different dimers (see Table 1). For instance, if an arbitrary dimer and a type 8 hexamer collide and a new dimer is created, this will be an acceptor homodimer only in one-third of all cases. It is equally probable that the created dimer will be a donor homodimer, or a heterodimer. Because in any case described by

Eq. 8 one of the three sorts of dimers must be expelled, the factors in front of a specific hexamer type sum to 1. This shows that $j_{\mathrm{AA}} + j_{\mathrm{DD}} + j_{\mathrm{DA}} = \Sigma_{\mathrm{T}=1}^{16} H_{\mathrm{T}} = c_{\mathrm{H}}$ must hold, which is also easily verified by Eqs. A11–A13.

After the establishment of the additional terms in Eqs. A8–A10, an approximate solution has to be obtained. Because of the equivalence between donors and acceptors and the constancy of the total dimer concentration, only the time evolution of the dimer concentration $[DA](t)$ needs to be considered, whereas the other two concentrations are given by $[AA](t) = [DD](t) = \frac{1}{2} ([AA] + [DD] + [DA]) - \frac{1}{2} [DA](t)$. Using $[A] \cdot [D] = \frac{1}{4} (([A] + [D])^2 - ([A] - [D])^2) = \frac{1}{4} ([A] + [D])^2$, rate Eq. A10 can be rewritten as

$$[D\dot{A}] = \frac{k_+}{2} ([A] + [D])^2 - (k_- + k_{\mathrm{dim}}c_{\mathrm{H}})[DA]$$
$$+ k_{\mathrm{dim}}([AA] + [DD] + [DA])j_{\mathrm{DA}}. \quad (A14)$$

Experimentally, it is clear that the 16 different hexamer concentrations that determine the fluorescence signal, and the term $j_{\mathrm{DA}}(t)$, are changing more slowly than the dimer concentrations. Therefore, Eq. A14 can be solved approximately for the very small time interval $t \in (0, \theta)$, where the "induction" period θ is so small that the hexamer concentrations remain nearly unchanged: $j_{\mathrm{DA}}(t) \approx j_{\mathrm{DA}}(0)$ for $t \in (0, \theta)$. For such a small time interval, all terms except $[DA]$ in Eq. A14 are constant, and the solution to Eq. A14 reads

$$[DA](t) = \left\{ [DA](0) \right.$$
$$\left. - \frac{k_+([A] + [D])^2/2 + k_{\mathrm{dim}}([AA] + [DD] + [DA])j_{\mathrm{DA}}(0)}{k_- + k_{\mathrm{dim}}c_{\mathrm{H}}} \right\}$$
$$\times \exp(-[k_- + k_{\mathrm{dim}}c_{\mathrm{H}}]t)$$
$$+ \frac{k_+([A] + [D])^2/2 + k_{\mathrm{dim}}([AA] + [DD] + [DA])j_{\mathrm{DA}}(0)}{k_- + k_{\mathrm{dim}}c_{\mathrm{H}}}$$
$$\text{for times } t \in (0, \theta). \quad (A15)$$

If now the dissociation rate of dimers k_- or, more precisely, $k_- + k_{\mathrm{dim}}c_{\mathrm{H}}$, is large enough for $\exp(-[k_- + k_{\mathrm{dim}}c_{\mathrm{H}}]\theta) \ll 1$, the first term proportional to the exponential function can be neglected at $t = \theta$, and one obtains

$$[DA](\theta)$$
$$\approx \frac{k_+([A] + [D])^2/2 + k_{\mathrm{dim}}([AA] + [DD] + [DA])j_{\mathrm{DA}}(0)}{k_- + k_{\mathrm{dim}}c_{\mathrm{H}}}. \quad (A16)$$

This value can now serve as the initial condition to integrate Eq. A14 for the next time interval from $t = \theta$ to $t = 2\theta$, and the solution reads

$$[DA](t) \approx \left\{ \frac{k_{\mathrm{dim}}([AA] + [DD] + [DA])}{k_- + k_{\mathrm{dim}}c_{\mathrm{H}}} [j_{\mathrm{DA}}(0) \right.$$
$$\left. - j_{\mathrm{DA}}(\theta)] \right\} \exp(-[k_- + k_{\mathrm{dim}}c_{\mathrm{H}}](t - \theta))$$
$$+ \frac{k_+([A] + [D])^2/2 + k_{\mathrm{dim}}([AA] + [DD] + [DA])j_{\mathrm{DA}}(\theta)}{k_- + k_{\mathrm{dim}}c_{\mathrm{H}}}$$
$$\approx \frac{k_+([A] + [D])^2/2 + k_{\mathrm{dim}}([AA] + [DD] + [DA])j_{\mathrm{DA}}(\theta)}{k_- + k_{\mathrm{dim}}c_{\mathrm{H}}},$$
$$\text{for times } t \in (\theta, 2\theta), \quad (A17)$$

where the last approximate equality follows because the change in j_{DA} during the time span τ has been assumed to be negligibly small: $j_{DA}(0) - j_{DA}(\theta) \approx 0$. Iterating this procedure allows one to obtain the approximate solution valid for all times longer than the induction period θ,

$$[DA](t)$$

$$\approx \frac{k_+([A] + [D])^2/2 + k_{dim}([AA] + [DD] + [DA])j_{DA}(t)}{k_- + k_{dim}c_H},$$

$$\text{for all } t > \theta. \quad \text{(A18)}$$

This equation expresses that the time dependence of the dimer concentrations is only governed by the slowly varying change in j_{DA}, i.e., $j_{DA}(t + \theta) \approx j_{DA}(t)$. Eq. A18 can be rewritten using the supposed equilibrium between monomers and dimers, $k_+([A] + [D])^2 = k_-([AA] + [DD] + [DA])$, which yields

$$[DA](t) \approx ([AA] + [DD] + [DA]) \frac{k_-/2 + k_{dim}j_{DA}(t)}{k_- + k_{dim}c_H}.$$

$$\text{(A19)}$$

The only assumption made so far is $\exp(-[k_- + k_{dim}c_H]\theta) \ll 1$, where θ is a small time interval during which the concentration changes of hexamers are negligible. This seems to be a very reasonable assumption, because the half-life period corresponding to k_- is on the order of 4.5×10^{-5} s, which is much shorter than the time over which the measured fluorescence signal changes, and even much shorter than the time that could be resolved experimentally. However, the next approximation has to be taken more seriously. Assuming that

$$k_- \gg 2k_{dim}c_H \quad \text{(A20)}$$

yields for the dimer concentration $[DA](t)$ in Eq. A19

$$[DA] \approx \frac{[AA] + [DD] + [DA]}{2} = \text{const.}, \quad \text{(A21a)}$$

and consequently for the other two concentrations,

$$[DD] \approx \frac{[AA] + [DD] + [DA]}{4} = \text{const.}, \quad \text{(A21b)}$$

$$[AA] \approx \frac{[AA] + [DD] + [DA]}{4} = \text{const.} \quad \text{(A21c)}$$

In terms of the lifetime of hexamers, condition Eq. A20 translates into

$$\tau_{dim} \gg \frac{2}{k_-} \frac{c_H}{([AA] + [DD] + [DA])} = \frac{2}{k_-} \cdot \frac{c_H}{c_D}. \quad \text{(A22)}$$

Taking the highest value for $c_D \cdot k_{dim}$ and, hence, the lowest for τ_{dim} from Table 3, which was determined for a total insulin concentration of 180 μM; approximating c_H by the upper limit $c_{total}/6$; and taking the value $k_- = 1.55 \times 10^4$ s^{-1} (Koren and Hammes, 1976) for the dissociation rate of dimers yields the following condition:

$$\tau_{dim} \geq 75 \text{ s} \gg (2/k_-) \cdot c_{total}/6c_D$$

$$= (2/1.55 \times 10^4 \text{ s}^{-1}) \cdot 180 \text{ }\mu\text{M}/6c_D$$

$$\Rightarrow c_D \gg 2 \cdot 180 \text{ }\mu\text{M}/(6 \cdot 1.55 \times 10^4 \text{ s}^{-1} \cdot 75 \text{ s})$$

$$= 0.052 \text{ nM}.$$

Thus, if the total dimer concentration is large enough to fulfill this condition, the slow time dependence of the three single dimer concentrations, [DD], [AA], and [DA], which is induced by the coupling to the hexamers,

can be neglected. To get an idea of the order of magnitude of c_D, the association constants of Hvidt (1991) for the R_6 case were taken to calculate the dimer concentration, resulting in 180 μM $\cdot$ 8%/2 = 7.2 μM, which is indeed orders of magnitude higher than 0.052 nM. Hence, Eqs. A21a,b,c could always consistently be assumed. Based on the assumption Eq. A22, the matrix $\underline{M}$ in Eq. 11b, which depends on the three dimer concentrations, or equivalently, on the three relative concentrations x_{AA}, x_{DD}, x_{DA}, is also constant. As a consequence, the set of 16 rate equations for the dimer model can easily be solved, using standard methods for a system of first-order differential equations with constant coefficients.

APPENDIX B

In this appendix the nonvanishing matrix elements of the matrices $\underline{M}_{mon}$ and $\underline{M}_{dim}$ are listed. ($(\underline{M})_{i,j}$ denotes the element in row i and column j.)

For the monomer model:

$$(\underline{M}_{mon})_{1,1} = -1/2, \quad (\underline{M}_{mon})_{1,2} = +1/12,$$

$$(\underline{M}_{mon})_{2,1} = +1/2, \quad (\underline{M}_{mon})_{2,2} = -1/2,$$

$$(\underline{M}_{mon})_{2,3} = +1/6, \quad (\underline{M}_{mon})_{2,4} = +1/6,$$

$$(\underline{M}_{mon})_{2,5} = +1/6, \quad (\underline{M}_{mon})_{2,6} = +1/6,$$

$$(\underline{M}_{mon})_{3,2} = +1/6, \quad (\underline{M}_{mon})_{3,3} = -1/2,$$

$$(\underline{M}_{mon})_{3,7} = +1/4, \quad (\underline{M}_{mon})_{3,8} = +1/12,$$

$$(\underline{M}_{mon})_{3,9} = +1/12, \quad (\underline{M}_{mon})_{3,10} = +1/12,$$

$$(\underline{M}_{mon})_{4,2} = +1/12, \quad (\underline{M}_{mon})_{4,4} = -1/2,$$

$$(\underline{M}_{mon})_{4,8} = +1/12, \quad (\underline{M}_{mon})_{4,9} = +1/12,$$

$$(\underline{M}_{mon})_{5,2} = +1/12, \quad (\underline{M}_{mon})_{5,5} = -1/2,$$

$$(\underline{M}_{mon})_{5,9} = +1/12, \quad (\underline{M}_{mon})_{5,10} = +1/12,$$

$$(\underline{M}_{mon})_{6,2} = +1/12, \quad (\underline{M}_{mon})_{6,6} = -1/2,$$

$$(\underline{M}_{mon})_{6,8} = +1/12, \quad (\underline{M}_{mon})_{6,10} = +1/12,$$

$$(\underline{M}_{mon})_{7,3} = +1/12, \quad (\underline{M}_{mon})_{7,7} = -1/2,$$

$$(\underline{M}_{mon})_{7,11} = +1/12,$$

$$(\underline{M}_{mon})_{8,3} = +1/12, \quad (\underline{M}_{mon})_{8,4} = +1/6,$$

$$(\underline{M}_{mon})_{8,6} = +1/6, \quad (\underline{M}_{mon})_{8,8} = -1/2,$$

$$(\underline{M}_{mon})_{8,11} = +1/12, \quad (\underline{M}_{mon})_{8,12} = +1/6,$$

$$(\underline{M}_{mon})_{8,14} = +1/6,$$

$$(\underline{M}_{mon})_{9,3} = +1/12, \quad (\underline{M}_{mon})_{9,4} = +1/6,$$

$$(\underline{M}_{mon})_{9,5} = +1/6, \quad (\underline{M}_{mon})_{9,9} = -1/2,$$

$$(\underline{M}_{mon})_{9,11} = +1/12, \quad (\underline{M}_{mon})_{9,12} = +1/6,$$

$$(\underline{M}_{mon})_{9,13} = +1/6,$$

$$(\underline{M}_{\text{mon}})_{10,3} = +1/12, \quad (\underline{M}_{\text{mon}})_{10,5} = +1/6,$$

$$(\underline{M}_{\text{mon}})_{10,6} = +1/6, \quad (\underline{M}_{\text{mon}})_{10,10} = -1/2,$$

$$(\underline{M}_{\text{mon}})_{10,11} = +1/12, \quad (\underline{M}_{\text{mon}})_{10,13} = +1/6,$$

$$(\underline{M}_{\text{mon}})_{10,14} = +1/6,$$

$$(\underline{M}_{\text{mon}})_{11,7} = +1/4, \quad (\underline{M}_{\text{mon}})_{11,8} = +1/12,$$

$$(\underline{M}_{\text{mon}})_{11,9} = +1/12, \quad (\underline{M}_{\text{mon}})_{11,10} = +1/12,$$

$$(\underline{M}_{\text{mon}})_{11,11} = -1/2, \quad (\underline{M}_{\text{mon}})_{11,15} = +1/6,$$

$$(\underline{M}_{\text{mon}})_{12,8} = +1/12, \quad (\underline{M}_{\text{mon}})_{12,9} = +1/12,$$

$$(\underline{M}_{\text{mon}})_{12,12} = -1/2, \quad (\underline{M}_{\text{mon}})_{12,15} = +1/12,$$

$$(\underline{M}_{\text{mon}})_{13,9} = +1/12, \quad (\underline{M}_{\text{mon}})_{13,10} = +1/12,$$

$$(\underline{M}_{\text{mon}})_{13,13} = -1/2, \quad (\underline{M}_{\text{mon}})_{13,15} = +1/12,$$

$$(\underline{M}_{\text{mon}})_{14,8} = +1/12, \quad (\underline{M}_{\text{mon}})_{14,10} = +1/12,$$

$$(\underline{M}_{\text{mon}})_{14,14} = -1/2, \quad (\underline{M}_{\text{mon}})_{14,15} = +1/12,$$

$$(\underline{M}_{\text{mon}})_{15,11} = +1/6, \quad (\underline{M}_{\text{mon}})_{15,12} = +1/6,$$

$$(\underline{M}_{\text{mon}})_{15,13} = +1/6, \quad (\underline{M}_{\text{mon}})_{15,14} = +1/6,$$

$$(\underline{M}_{\text{mon}})_{15,15} = -1/2, \quad (\underline{M}_{\text{mon}})_{15,16} = +1/2,$$

$$(\underline{M}_{\text{mon}})_{16,15} = +1/12, \quad (\underline{M}_{\text{mon}})_{16,16} = -1/2.$$

For the dimer model:

$$(\underline{M}_{\text{dim}})_{1,1} = -3/4, \quad (\underline{M}_{\text{dim}})_{1,2} = +1/12,$$

$$(\underline{M}_{\text{dim}})_{1,4} = +1/12,$$

$$(\underline{M}_{\text{dim}})_{2,1} = +1/2, \quad (\underline{M}_{\text{dim}})_{2,2} = -2/3,$$

$$(\underline{M}_{\text{dim}})_{2,3} = +1/6, \quad (\underline{M}_{\text{dim}})_{2,4} = +1/6,$$

$$(\underline{M}_{\text{dim}})_{2,5} = +1/6, \quad (\underline{M}_{\text{dim}})_{2,6} = +1/6,$$

$$(\underline{M}_{\text{dim}})_{2,8} = +1/12, \quad (\underline{M}_{\text{dim}})_{2,9} = +1/12,$$

$$(\underline{M}_{\text{dim}})_{3,2} = +1/6, \quad (\underline{M}_{\text{dim}})_{3,3} = -3/4,$$

$$(\underline{M}_{\text{dim}})_{3,5} = +1/6, \quad (\underline{M}_{\text{dim}})_{3,6} = +1/6,$$

$$(\underline{M}_{\text{dim}})_{3,7} = +1/4, \quad (\underline{M}_{\text{dim}})_{3,8} = +1/12,$$

$$(\underline{M}_{\text{dim}})_{1,2} = +1/12,$$

$$(\underline{M}_{\text{dim}})_{3,9} = +1/12, \quad (\underline{M}_{\text{dim}})_{3,10} = +1/12,$$

$$(\underline{M}_{\text{dim}})_{3,11} = +1/12,$$

$$(\underline{M}_{\text{dim}})_{4,1} = +1/4, \quad (\underline{M}_{\text{dim}})_{4,2} = +1/12,$$

$$(\underline{M}_{\text{dim}})_{4,4} = -3/4, \quad (\underline{M}_{\text{dim}})_{4,8} = +1/12,$$

$$(\underline{M}_{\text{dim}})_{4,9} = +1/12, \quad (\underline{M}_{\text{dim}})_{4,12} = +1/6,$$

$$(\underline{M}_{\text{dim}})_{5,2} = +1/12, \quad (\underline{M}_{\text{dim}})_{5,3} = +1/12,$$

$$(\underline{M}_{\text{dim}})_{5,5} = -3/4, \quad (\underline{M}_{\text{dim}})_{5,9} = +1/12,$$

$$(\underline{M}_{\text{dim}})_{5,10} = +1/12, \quad (\underline{M}_{\text{dim}})_{5,14} = +1/12,$$

$$(\underline{M}_{\text{dim}})_{6,2} = +1/12, \quad (\underline{M}_{\text{dim}})_{6,3} = +1/12,$$

$$(\underline{M}_{\text{dim}})_{6,6} = -3/4, \quad (\underline{M}_{\text{dim}})_{6,8} = +1/12,$$

$$(\underline{M}_{\text{dim}})_{6,10} = +1/12, \quad (\underline{M}_{\text{dim}})_{6,13} = +1/12,$$

$$(\underline{M}_{\text{dim}})_{7,3} = +1/12, \quad (\underline{M}_{\text{dim}})_{7,7} = -3/4,$$

$$(\underline{M}_{\text{dim}})_{7,10} = +1/12, \quad (\underline{M}_{\text{dim}})_{7,11} = +1/12,$$

$$(\underline{M}_{\text{dim}})_{8,2} = +1/12, \quad (\underline{M}_{\text{dim}})_{8,3} = +1/12,$$

$$(\underline{M}_{\text{dim}})_{8,4} = +1/6, \quad (\underline{M}_{\text{dim}})_{8,5} = +1/12,$$

$$(\underline{M}_{\text{dim}})_{8,6} = +1/12, \quad (\underline{M}_{\text{dim}})_{8,8} = -2/3,$$

$$(\underline{M}_{\text{dim}})_{8,11} = +1/12,$$

$$(\underline{M}_{\text{dim}})_{8,12} = +1/6, \quad (\underline{M}_{\text{dim}})_{8,13} = +1/12,$$

$$(\underline{M}_{\text{dim}})_{8,14} = +1/12, \quad (\underline{M}_{\text{dim}})_{8,15} = +1/12,$$

$$(\underline{M}_{\text{dim}})_{9,2} = +1/12, \quad (\underline{M}_{\text{dim}})_{9,3} = +1/12,$$

$$(\underline{M}_{\text{dim}})_{9,4} = +1/6, \quad (\underline{M}_{\text{dim}})_{9,5} = +1/12,$$

$$(\underline{M}_{\text{dim}})_{9,6} = +1/12, \quad (\underline{M}_{\text{dim}})_{9,9} = -2/3,$$

$$(\underline{M}_{\text{dim}})_{9,11} = +1/12,$$

$$(\underline{M}_{\text{dim}})_{9,12} = +1/6, \quad (\underline{M}_{\text{dim}})_{9,13} = +1/12,$$

$$(\underline{M}_{\text{dim}})_{9,14} = +1/12, \quad (\underline{M}_{\text{dim}})_{9,15} = +1/12,$$

$$(\underline{M}_{\text{dim}})_{10,3} = +1/12, \quad (\underline{M}_{\text{dim}})_{10,5} = +1/6,$$

$$(\underline{M}_{\text{dim}})_{10,6} = +1/6, \quad (\underline{M}_{\text{dim}})_{10,7} = +1/4,$$

$$(\underline{M}_{\text{dim}})_{10,10} = -7/12, \quad (\underline{M}_{\text{dim}})_{10,11} = +1/12,$$

$$(\underline{M}_{\text{dim}})_{10,13} = +1/6, \quad (\underline{M}_{\text{dim}})_{10,14} = +1/6,$$

$$(\underline{M}_{\text{dim}})_{11,3} = 1/12, \quad (\underline{M}_{\text{dim}})_{11,7} = 1/4,$$

$$(\underline{M}_{\text{dim}})_{1,2} = +1/12, \quad (\underline{M}_{\text{dim}})_{11,8} = +1/12,$$

$$(\underline{M}_{\text{dim}})_{11,9} = +1/12, \quad (\underline{M}_{\text{dim}})_{11,10} = +1/12,$$

$$(\underline{M}_{\text{dim}})_{11,11} = -3/4, \quad (\underline{M}_{\text{dim}})_{11,13} = +1/6,$$

$$(\underline{M}_{\text{dim}})_{11,14} = +1/6, \quad (\underline{M}_{\text{dim}})_{11,15} = +1/6,$$

$$(\underline{M}_{\text{dim}})_{12,4} = +1/6, \quad (\underline{M}_{\text{dim}})_{12,8} = +1/12,$$

$$(\underline{M}_{\text{dim}})_{12,9} = +1/12, \quad (\underline{M}_{\text{dim}})_{12,12} = -3/4,$$

$$(\underline{M}_{\text{dim}})_{12,15} = +1/12, \quad (\underline{M}_{\text{dim}})_{12,6} = +1/4,$$

$$(\underline{M}_{\mathrm{dim}})_{13,6} = +1/12, \quad (\underline{M}_{\mathrm{dim}})_{13,9} = +1/12,$$

$$(\underline{M}_{\mathrm{dim}})_{13,10} = +1/12, \quad (\underline{M}_{\mathrm{dim}})_{13,11} = +1/12,$$

$$(\underline{M}_{\mathrm{dim}})_{13,13} = -3/4, \quad (\underline{M}_{\mathrm{dim}})_{13,15} = +1/12,$$

$$(\underline{M}_{\mathrm{dim}})_{14,5} = +1/12, \quad (\underline{M}_{\mathrm{dim}})_{14,8} = +1/12,$$

$$(\underline{M}_{\mathrm{dim}})_{14,10} = +1/12, \quad (\underline{M}_{\mathrm{dim}})_{14,11} = +1/12,$$

$$(\underline{M}_{\mathrm{dim}})_{14,14} = -3/4, \quad (\underline{M}_{\mathrm{dim}})_{14,15} = +1/12,$$

$$(\underline{M}_{\mathrm{dim}})_{15,8} = +1/12, \quad (\underline{M}_{\mathrm{dim}})_{15,9} = +1/12,$$

$$(\underline{M}_{\mathrm{dim}})_{15,11} = +1/6, \quad (\underline{M}_{\mathrm{dim}})_{15,12} = +1/6,$$

$$(\underline{M}_{\mathrm{dim}})_{15,13} = +1/6, \quad (\underline{M}_{\mathrm{dim}})_{15,14} = +1/6,$$

$$(\underline{M}_{\mathrm{dim}})_{15,15} = -2/3, \quad (\underline{M}_{\mathrm{dim}})_{15,16} = +1/2,$$

$$(\underline{M}_{\mathrm{dim}})_{16,12} = +1/12, \quad (\underline{M}_{\mathrm{dim}})_{16,15} = +1/12,$$

$$(\underline{M}_{\mathrm{dim}})_{16,16} = -3/4.$$

REFERENCES

Anderson, S., and G. Weber. 1966. The reversible acid dissociation and hybridization of lactic dehydrogenase. *Arch. Biochem. Biophys.* 116:207–223.

Bakaysa, D. L., J. Radziuk, H. A. Havel, M. L. Brader, S. Li, S. W. Dodd, J. M. Beals, A. H. Pekar, and D. N. Brems. 1996. Physicochemical basis for the rapid time-action of Lys^{B28}Pro^{B29}-insulin: dissociation of a protein-ligand complex. *Protein Sci.* 5:2521–2531.

Baker, E. N., T. L. Blundell, J. F. Cutfield, S. M. Cutfield, E. J. Dodson, G. G. Dodson, D. M. Crowfoot Hodgkin, R. E. Hubbard, N. W. Isaacs, C. D. Reynolds, K. Sakabe, N. Sakabe, and N. M. Vijayan. 1988. The structure of 2Zn pig insulin crystals at 1.5 Å resolution. *Philos. Trans. R. Soc. Lond. B.* 319:369–456.

Bentley, G., E. J. Dodson, G. G. Dodson, D. Hodgkin, and D. A. Mercola. 1976. Structure of insulin in 4-zinc insulin. *Nature.* 261:166–168.

Bentley, G. A., G. G. Dodson, E. J. Dodson, D. C. Hodgkin, D. A. Mercola, and A. Wollmer. 1975. Structural rearrangements in insulin: a comparison of 2 and 4 zinc insulin structures. British Diabetes Association, Medical and Scientific Section, Spring Meeting 1975, Sheffield.

Blundell, T. L., G. G. Dodson, D. C. Hodgkin, and D. A. Mercola. 1972. Insulin: the structure in the crystal and its reflection in chemistry and biology. *Adv. Protein Chem.* 26:279–402.

Brange, J. 1994. Stability of Insulin. Kluwer Academic Publishers, Boston.

Coffman, F. D., and M. F. Dunn. 1988. Insulin-metal ion interactions: the binding of divalent cations to insulin hexamers and tetramers and the assembly of insulin hexamers. *Biochemistry.* 27:6179–6187.

De Graaf, R. A. G., A. Lewit-Bentley, and S. P. Tolley. 1981. Effects of destabilizing agents on the insulin hexamer structure. *In* Structural Studies on Molecules of Biological Interest. G. G. Dodson, J. P. Glusker, and D. Sayre, editors. Clarendon Press, Oxford. 547–556.

Derewenda, U., Z. Derewenda, E. J. Dodson, G. G. Dodson, R. D. Reynolds, G. D. Smith, C. Sparks, and D. Swenson. 1989. Phenol stabilizes more helix in a new symmetrical zinc insulin hexamer. *Nature.* 338:594–596.

Dodson, G. G., and D. Steiner. 1998. The role of assembly in insulin's biosynthesis. *Curr. Opin. Struct. Biol.* 8:189–194.

Ducommun, Y., and A. E. Merbach. 1986. Solvent exchange reactions. *In* Inorganic High Pressure Chemistry. R. van Eldik, editor. Elsevier, Amsterdam. 69–113.

Eigen, M. 1963. Fast elementary steps in chemical reaction mechanisms. *Pure Appl. Chem.* 6:97–115.

Eisenstein, E., and H. K. Schachman. 1989. Determining the roles of subunits in protein function. *In* Protein Function—A Practical Approach. T. E. Creighton, editor. IRL Press, Oxford. 135–176.

Erijman, L., and G. Weber. 1991. Oligomeric protein associations: transition from stochastic to deterministic equilibrium. *Biochemistry.* 30:1595–1599.

Erijman, L., and G. Weber. 1993. Use of sensitized fluorescence for the study of the exchange of subunits in protein aggregates. *Photochem. Photobiol.* 57:411–415.

Förster, T. 1948. Zwischenmolekulare Energiewanderung und Fluoreszenz. *Ann. Phys.* 2:55–75.

Gross, L., and M. F. Dunn. 1992. Spectroscopic evidence for an intermediate in the T6 to R6 allosteric transition of the Co(II)-substituted insulin hexamer. *Biochemistry.* 31:1295–1301.

Hassiepen, U., M. Federwisch, T. Mülders, V. J. Lenz, H. G. Gattner, P. Krüger, and A. Wollmer. 1998. Analysis of protein self-association at constant concentration by fluorescence-energy transfer. *Eur. J. Biochem.* 255:580–587.

Hvidt, S. 1991. Insulin association in neutral solutions studied by light scattering. *Biophys. Chem.* 39:205–213.

Jacoby, E., Q. X. Hua, A. S. Stern, B. H. Frank, and M. A. Weiss. 1996. Structure and dynamics of a protein assembly. ^{1}H-NMR studies of the 36 kDa R_6 insulin hexamer. *J. Mol. Biol.* 258:136–157.

Jaenicke, R. 1987. Folding and association of proteins. *Prog. Biophys. Mol. Biol.* 49:117–237.

Jaenicke, R., R. Koberstein, and B. Teuscher. 1971. The enzymically active unit of lactic dehydrogenase. Molecular properties of lactic dehydrogenase at low-protein and high salt concentrations. *Eur. J. Biochem.* 23:150–159.

Jaenicke, R., and R. Rudolph. 1986. Refolding and association of oligomeric proteins. *Methods Enzymol.* 131:218–250.

Kaarsholm, N. C., H. C. Ko, and M. F. Dunn. 1989. Comparison of solution structural flexibility and zinc binding domains for insulin, proinsulin, and miniproinsulin. *Biochemistry.* 28:4427–4435.

Koren, R., and G. G. Hammes. 1976. A kinetic study of protein-protein interactions. *Biochemistry.* 15:1165–1171.

Krüger, P., G. Gilge, Y. Cabuk, and A. Wollmer. 1990. Cooperativity and intermediate states in the T → R-structural transformation of insulin. *Biol. Chem. Hoppe-Seyler.* 371:669–673.

Lenz, V. J., H. G. Gattner, M. Leithäuser, D. Brandenburg, A. Wollmer, and H. Höcker. 1994. Proteolyses of a fluorogenic insulin derivative and native insulin in reversed micelles monitored by fluorescence emission, reversed-phase high-performance liquid chromatography, and capillary zone electrophoresis. *Anal. Biochem.* 221:85–93.

Levine, I. N. 1995. Physical Chemistry. McGraw-Hill, New York.

Meighen, E. A., V. Pigiet, and H. K. Schachman. 1970. Hybridization of native and chemically modified enzymes. 3. The catalytic subunits of aspartate transcarbamylase. *Proc. Natl. Acad. Sci. USA.* 65:234–241.

Nicholls, A., K. A. Sharp, and B. Honig. 1991. Protein folding and association: insights from the interfacial and thermodynamic properties of hydrocarbons. *Proteins.* 11:281–296.

Osborne, H. H., and M. R. Hollaway. 1974. The hybridization of glyceraldehyde 3-phosphate dehydrogenases from rabbit muscle and yeast. Kinetics and thermodynamics of the reaction and isolation of the hybrid. *Biochem. J.* 143:651–662.

Palmieri, R., R. W. Lee, and M. F. Dunn. 1988. ^{1}H Fourier transform NMR studies of insulin: coordination of Ca^{2+} to the Glu(B13) site drives hexamer assembly and induces a conformation change. *Biochemistry.* 27:3387–3397.

Peterman, B. F. 1979. Measurement of the dead time of a fluorescence stopped-flow instrument. *Anal. Biochem.* 93:442–444.

Price, N. C. 1994. Assembly of multi-subunit structures. *In* Mechanisms of Protein Folding. R. H. Pain, editor. IRL Press, Oxford. 160–193.

Rahuel-Clermont, S., C. A. French, N. C. Kaarsholm, M. F. Dunn, and C. I. Chou. 1997. Mechanisms of stabilization of the insulin hexamer through allosteric ligand interactions. *Biochemistry.* 36:5837–5845.

Ramesh, V., and J. H. Bradbury. 1986. ^{1}H N.M.R. studies of insulin. Reversible transformation of 2-zinc to 4-zinc insulin hexamer. *Int. J. Pept. Protein Res.* 28:146–153.

Renscheidt, H., W. Strassburger, U. Glatter, A. Wollmer, G. G. Dodson, and D. A. Mercola. 1984. A solution equivalent of the 2Zn → 4Zn transformation of insulin in the crystal. *Eur. J. Biochem.* 142:7–14.

Roy, M., M. L. Brader, R. W. Lee, N. C. Kaarsholm, J. F. Hansen, and M. F. Dunn. 1989. Spectroscopic signatures of the T to R conformational transition in the insulin hexamer. *J. Biol. Chem.* 264:19081–19085.

Schlichtkrull, J. 1958. Insulin Crystals. Munksgard, Copenhagen.

Schulzki, H. D., B. Kramer, J. Fleischhauer, D. A. Mercola, and A. Wollmer. 1990. Calcium-dependent distance changes in binary and ternary complexes of troponin. *Eur. J. Biochem.* 189:683–692.

Smith, G. D., and G. G. Dodson. 1992. The structure of a rhombohedral R6 insulin hexamer that binds phenol. *Biopolymers.* 32:441–445.

Smith, G. D., W. L. Duax, E. J. Dodson, G. G. Dodson, R. A. G. de Graaf, and C. D. Reynolds. 1982. The structure of des-Phe B1 bovine insulin. *Acta Crystallogr. B.* 38:3028–3032.

Sundberg, R. J., and R. B. Martin. 1974. Interactions of histidine and other imidazole derivatives with transition metal ions in chemical and biological systems. *Chem. Rev.* 74:471–517.

Thomas, B., and A. Wollmer. 1989. Cobalt probing of structural alternatives for insulin in solution. *Biol. Chem. Hoppe-Seyler.* 370:1235–1244.

Wollmer, A., B. Rannefeld, B. R. Johansen, K. R. Hejnaes, P. Balschmidt, and F. B. Hansen. 1987. Phenol-promoted structural transformation of insulin in solution. *Biol. Chem. Hoppe-Seyler.* 368:903–911.

Yang, Y. R., and H. K. Schachman. 1987. Hybridization as a technique for studying interchain interactions in the catalytic trimers of aspartate transcarbamoylase. *Anal. Biochem.* 163:188–195.